Evaluation of Microcrystalline Cellulose isolated from Mango (mangofera indica) kernel as Directly Compressible Pharmaceutical Excipient

DERSO TEJU (B.Pharm)

OCTOBER, 2024

MEKELLE, ETHIOPI

Evaluation of Microcrystalline Cellulose isolated from Mango (mangofera indica) kernel as Directly Compressible Pharmaceutical Excipient

DERSO TEJU(B.Pharm)

A Thesis Submitted to the Department of Pharmaceutics, School of Pharmacy, College of Health Sciences, Mekelle University in Partial Fulfillment of the Requirements for the Degree of Master of Science in Pharmaceutics

Under the Supervision of: Mr. Yohannes Reda (B.Pharm, M.Sc. in Pharmaceutics)

Mrs. Tsadkan G/meskel (B.Pharm, M.Sc. in Pharmaceutics)

October, 2024

Mekelle, Ethiopia

DECLARATION

I, the undersigned, declare that the thesis entitled " Isolation, Characterization and Evaluation of Microcrystalline Cellulose from Mango kernel as Directly Compressible Pharmaceutical Excipient" is a result of my investigation and has not been done in substance for the award of any degree in any other university. All sources of the materials used in this thesis have appropriately been acknowledged.

Name …….. Signature …….. Date……..

CERTIFICATE

This is to certify that the thesis submitted in partial fulfillment of the requirements for the Degree of Masters of Science in Pharmaceutics by ‘ **Derso Teju**, entitled “ Evaluation of Microcrystalline Cellulose isolated from Mango kernel as Directly Compressible Pharmaceutical Excipient ” complies with the regulations of the University and meets the accepted standards concerning originality and quality.

Signed by the following examining committee**:**

Signature **Date**

1 Mr. Yohanes Reda

(Advisor)

2 Mrs. Tsadkan G/meskel

(Advisor)

3 G/michael Mulu

(External Examiner)

4 Afewerk Getachew

(Internal Examiner**)**

The Department of Pharmaceutics, School of Pharmacy, College of Health Sciences, Mekelle University

ACKNOWLEDGMENTS

At the very beginning, I want to express my heartfelt gratitude to the almighty God for his infinite love and blessings throughout my life.

I wish to express my sincere gratitude to my supervisors, Mr. Yohannes and Mrs. Tsadkan G/meskel , for their guidance, encouragement and insightful comments throughout the research work. They helped me to understand and enrich my research work.

I am highly thankful to Ethiopian Pharmaceuticals Manufacturing Share Company (EPHARM) for providing me paracetamol and for allowing me to access tablet compression machine. I also would like to acknowledge Bahirdar University Institute of Textile for FTIR and TGA studies. I am thankful to Adama Science and Technology University, Department of Applied Biology, for SEM study and Department of Materials Science Engineering, for XRD analysis; I am also thankful to Addis Ababa University for Laser diffraction particle size analysis.

I also thank all my classmates and staff members of Department of Pharmaceutics for their helpful collaboration and friendship during the time of research. I would like to acknowledge Mekelle University and the University of Gondar for sponsoring my postgraduate study.

TABLE OF CONTENTS

LIST OF FIGURES

LIST OF TABLES

ABBREVIATIONS/ ACRONYMS

AGU	D-anhydroglucopyranose units
BP	British Pharmacopoeia
CF	Compression Force
CI	Compressibility index
Cuam	Cuprammonium hydroxide
DC	Direct compression
DP	Degree of polymerization
DTG	Differential thermal analysis
FTIR	Fourier Transform Infrared Spectroscopy
HR	Hausner ratio
LSR	Lubricant sensitivity ratio
MCC	Microcrystalline Cellulose
MK-MCC	Mango kernel microcrystalline cellulose
NF	National Formulary
RH	Relative humidity
SEM	Scanning electron microscopy
TGA	Thermogravimetric Analysis
USP	United States Pharmacopoeia
UV	Ultraviolet - Visible
XRD	X-ray Diffraction

ABSTRACT

Background: Cellulose, obtained predominantly from wood and cotton, stands as the most abundant natural polymer on earth. The consumption of cellulose for various industrial application is continuously increasing worldwide. The extraction of cellulose from agricultural waste addresses critical issues by enhancing efficient resource utilization, minimizing waste, and reducing the environmental impacts associated with deforestation. Therefore, a sustainable enviroment may be established by using the abundant agricultural waste from plant fibers. Mango is one of the main fruit crops produced and exported in Ethiopia. Therefore, this work aimed to prepare and characterize mango kernel microcrystalline cellulose (MK-MCC) and assess it as directly compressible pharmaceutical excipient.

Method: Mango kernel cellulose was extracted using NaOH treatments, then cellulose was hydrolyzed by HCl to prepare mango kernel microcrystalline cellulose. The isolated MCC was characterized through scanning electron microscope, Fourier Transform infrared spectroscopy, Laser diffraction, thermogravimetric analysis and x-ray diffraction and compared with Avicel PH 101. The mechanical properties of both plain MK-MCC tablets and model drug (paracetamol) containing MK-MCC tablets were evaluated and compared with standard Avicel PH 101 tablets.

Results: Cellulose and MCC yield on the dry weight basis of mango kernel were found to be 36.5% ± 1.57 and 28.64% ±1.66 respectively. Crystallinity index (CrI) of Mango kernel cellulose was 76.5%. Scanning electron microscopy also showed MK-MCC had smooth surface morphology, irregular and rod-shaped fiber strands. The MK-MCC powders exhibited a bimodal, moderate particle size distribution. The physicochemical studies of MK-MCC revealed moisture content 3.47% w/w, ash value (0.07), pH (5.97), water soluble substances (0.14%) and ether soluble substances (0.03%) that were all within the allowable limit of USP 30/NF 25. MK-MCC preparations showed lower crushing and tensile strengths than Avicel PH-101. MK-MCC effectively incorporated 50% paracetamol in a tablet formulation suitable for direct compression.

Conclusion: Based on the results of this study mango kernel could be a promising locally available potential source of cellulose and MCC for pharmaceutical applications.

Keywords: Cellulose, mango keernel, Microcrystalline cellulose, direct compression.

1. INTRODUCTION

The increasing demand for sustainable and cost-effective pharmaceutical excipients has driven researchers to investigate alternative sources of microcrystalline cellulose (MCC). Using agricultural waste as a source MCC offers a novel approach to meet the growing need for sustainable, affordable, and biocompatible excipients in pharmaceutical formulations. Depletion of plant-based materials and unanticipated environmental changes are caused by the increasing human population and exploitation of plant resources. This problem is made worse by the fact that many important natural resources are wasted as a result of the incomplete use of plant components (fruit, seed, roots, stem, leaves, etc.). However, transforming these agricultural waste into valuable pharmaceutical excipients offers numerous environmental, economical, and technological benefits. By replacing wood-based cellulose with agricultural waste based cellulose, the need for deforestation is minimized, contributing to the conservation of natural ecosystems and helping to combat climate change. This provides pharmaceutical manufacturers a cost-effective way to produce excipients without relying on more expensive materials. Thus, maximizing the use of plant components for human benefit and environmental conservation is imperative. This has received much attention from scientists and researchers to apply it in developing biodegradable composite products (Asif et al., 2022).

An abundant, affordable, and easily accessible source of renewable lignocellulosic biomass is provided by renewable agricultural wastes. The most abundant renewable organic material on earth is natural lignocellulose. From the forest to the sea, there is an enormous and wide diversity of biomass, and photosynthesis continuously produces new biomass. Both wood and non-wood lignocellulosic biomass are excellent raw materials for production of polymers and composites production. Nevertheless, when considering an environmental approach, non-woody lignocellulosic biomass is preferred. Non-wood lignocellulosic biomass is abundant, inexpensive, easy to process and has a short growth and harvest period; therefore, it is introduced as a potential for cellulose production (Senusi et al., 2020).

1.1. Cellulose

Cellulose is one of the most abundant renewable biodegradable polymer resource for multifunctional porposes. It can be obtained from a vast number of sources such as cell walls of wood and plants, some species of bacteria, and algae, as well as tunicates, which are the only known cellulose-containing animals (Lavanya et al., 2011).

Cell walls primarily comprise cellulose, hemicellulose, and lignin in approximate ratios of 4:3:3. This ratio varies among different sources, including hardwoods, softwoods, and herbs. In addition to these three main components, natural lignocellulosic materials include minor amounts of pectin, nitrogenous compounds, and trace amounts of ash (Rowell et al., 2005)

Lignin is an amorphous phenolic polymer with a three-dimensional structure. It is mainly formed from three types of hydroxycinnamyl alcohols—p-coumaryl alcohol, coniferyl alcohol, and sinapyl alcohol—through a process that involves the generation of free radicals and subsequent chemical coupling reactions. Based on its aromatic core, lignin's phenylpropane units are categorized into guaiacyl propane, syringyl propane, and p-hydroxyphenyl propane. In straw lignin, guaiacyl propane and syringyl propane are the predominant types, with only a small amount of p-hydroxyphenyl propane present. In addition to the strong hydrogen bonding internally in the lignin, there exists a stable lignin-carbohydrate complex. Lignin provides structural stability, impermeability, and resistance against microbial attack by connecting the components of the main cell wall (Kalia et al., 2014).

Hemicellulose is a heterogeneous glucan with a short side chain composed of two or more monosaccharides. Hemicellulose is composed of various units, which can include pentose sugars like arabinose and xylose, hexose sugars such as mannose, glucose, and galactose, as well as uronic acids, including α-D-glucuronic acid, α-D-galacturonic acid, and α-D-4-O-methylgalacturonic acid. Hemicellulose is an amorphous material, typically exhibits a low degree of polymerization, mostly below 200. Generally, hemicellulose is the most complex of the components in the cell wall of lignocellulose, because since it forms covalent bonds (mainly -benzyl ether linkages) with lignin and an ester linkage with acetyl units and hydroxycinnamic acids (Spiridon and Popa, 2008).

Cellulose is a semicrystalline polymer consisting of a linear homopolymer of D-glucopyranose residues ($C_6H_{11}O_5$) connected by β-(1-4)-glycosidic linkages. In each anhydroglucose unit (AGU) of the cellulose chain, there are three reactive hydroxyl groups: a primary hydroxyl group at C6 and two secondary hydroxyl groups at C2 and C3, which are situated in the plane of the ring and can form intra and intermolecular hydrogen bonds. Therefore, due to this chemical constitution and spatial conformation, cellulose often presents a highly ordered structure. The reducing and non-reducing end groups are also present in the cellulose molecule. A free hemiacetal (aldehyde) is present at position C-1 in the reducing end group, whereas a free hydroxyl group is present at position C-4 in the non-reducing end group (Heise et al., 2021).

Different hydrogen bonding systems are present in cellulose, and these systems have a significant influence on its characteristics. For example, the hydroxyl groups' reactivity, poor solubility in most solvents, and crystallinity originated from strong hydrogen bond systems. Cellulose also contains hydrophobic regions, particularly around the carbon atoms, which influence its overall properties, including solubility (Kondo, 2005).

The hydroxyl groups of the AGU, the oxygen atoms in the D-glucopyranose ring, and the glycosidic linkage interact within the chain or with other cellulose chains through the formation of both intramolecular and intermolecular hydrogen bonds. These hydrogen bonds lead to the formation of various three-dimensional structures (Kondo, 2005)

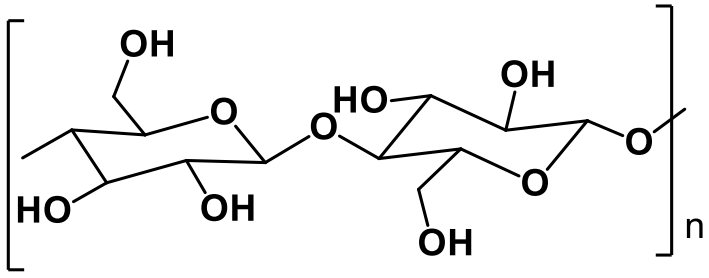

Figure 1: Molecular structure of cellulose (Heinze, 2016).

Degree of polymerization (DP) is the convenient way of expressing the molecular size of polymer molecules, which represents the number of glucose units present in the cellulose chain. The DP of cellulose varies depending on the source and the processing methods used. Temperature, acid concentration, and time are the factors that determine how exponentially the DP of cellulose drops during acid hydrolysis. For example, cellulose typically has a DP greater than 440, while microcrystalline cellulose (MCC) has a DP of less than 350, making DP a useful criterion for distinguishing between the two (Chaerunisaa et al., 2019).

The viscometric technique is the most widely used, cost-effective, and straightforward method for measuring the DP of cellulose. This involves dissolving the cellulose sample in solvents like cuprammonium hydroxide (Cuam) or copper ethylenediamine for analysis (Oberlerchner et al., 2015).

Depending on the source, the majority of cellulosic materials are composed of crystalline and amorphous domains in different proportions. The crystalline domain of cellulose, which constitutes the organized and majority portion, forms due to interactions between glucose chains via van der Waals forces and hydrogen bonding. In contrast, the amorphous cellulose, which constitutes a smaller proportion, is less ordered and more prone to chemical degradation. The amorphous regions are more susceptible to hydrolysis when exposed to high concentrations of mineral acids, as their disorganized structure allows easier access for the acid to break down the polymer chains (Ciolacu et al., 2011).

The ratio of the mass of crystalline domains and the total mass of cellulose is expressed as degree of crystallinity that can be determined either by X-Ray Diffractometer (XRD) or infrared spectroscopy. Degree of crystallinity is more dependent on pulp source rather than on processing conditions. The degree of crystallinity of cellulose greatly affects its physico-chemical characteristics. MCC is characterized by a high degree of crystallinity ranging between 60% and 80% (Salem et al., 2023).

Native cellulose (also called cellulose I) exists in two different crystal forms: cellulose Iα and cellulose Iβ. Cellulose Iβ is a monoclinic allomorph that is commonly observed in plant cellulose, while cellulose Iα is a triclinic allomorph generally found in algae and bacterial cellulose. As a result, cellulose derived from various biomasses exhibits a range of crystalline

characteristics. The crystal structure of native cellulose can be converted to that of cellulose II by NaOH treatment. The main characteristics of cellulose are white, tasteless, odorless, semi crystalline, hydrophobic (Gupta et al., 2019).

1.2. Sources of cellulose

Cellulose is a naturally abundant polysaccharide and can be sourced from a variety of plant-based materials. Traditionally, cotton and wood pulp have been the principal sources of cellulose. Cotton, with a cellulose content of about 90%, and wood, which contains approximately 40% to 50% cellulose, are the most widely used sources in industrial applications. Cellulose can be isolated from various agricultural waste resources such as soybean hulls, pea hull, corn bran, dried beet pulp, and oat hull ,rice straw, wheat straw, corn stalks (Sundarraj and Ranganathan, 2018), oil palm empty fruit bunch (Haafiz et al., 2014), Cocoa Pod Husk (Adeleye et al., 2022), Teff Straw (Getachew et al., 2023), coffe husk (Collazo-Bigliardi et al., 2018), orange mesocarp (Ejikeme, 2008), sugarcane bagasse. Some species of algae, particularly green algae, also produce cellulose, which is used for specific purposes such as biodegradable materials. Grasses, including sugarcane, and flax are also rich in cellulose (Katakojwala and Mohan, 2020).

Cellulose constitutes approximately 33% of all plant material, with cotton containing about 90% and wood ranging from 40% to 50%. Large volumes of cellulosic waste are produced annually by a variety of agricultural waste products. Finding new use for these "agricultural cellulosic wastes" is highly desired. There is a strong need to put these "agricultural cellulosic wastes" to alternative applications. The chemical analysis of different plant fiber revealed different yields of cellulose. The percentage yields from different agricultural by-products are: coconut husk (44.84%), pea peels (50%), cucumber peels (65.55%), corn husk (42%), corn cob (33%), lupine husk (36%), and coffee husk (35.5%). These diverse sources make cellulose a widely available and renewable material, serving a range of industries from pharmaceutical to textiles (Gabriel et al., 2020).

1.3. Mango plants

Mangoes are one of the top five tropical fruits in the world found in more than 100 nations. They grow best in tropical and subtropical climates, however they can also grow in a broad range of climate condition. The Mangifera genus comprises about 40 species, of which at least 26 are known to produce edible fruits. The most common species in this genus is Mangifera indica, or the common mango, which is cultivated in many tropical regions. It is widely cultivated in India, China, Thailand, Indonesia, Philippines, Brazil, Pakistan, and Mexico (Tharanathan et al., 2006).

Mango is one of the main fruit crops produced and exported from Ethiopia. It is both significant as commercially and as a subsistence crop for family farms. In Ethiopia, mango cultivation is primarily found in the western and eastern regions of Oromia, as well as in SNNPR, Benishangul, and Amhara. These areas have favorable climates for mango farming, characterized by warm temperatures and well-distributed rainfall, which contribute to the fruit's growth and quality (Honja, 2014).

A significant quantity of mango by-products is generated during fruit processing, leading to a major disposal issue that can pose environmental risks and result in economic losses for the fruit processing industry. These by-products, including mango peels, seeds, and pits, are often discarded or burned, contributing to pollution and waste (Jahurul et al., 2015).

Mango fruit consists of several key components, including mesocarp, exocarp, and endocarp (Figure 2). These components, along with the seed, collectively form the mature fruit. The mesocarp (known as pulp) is the most consumed part of thefruit and consists of 33-85% of the fruit mass. The exocarp corresponds to the peel and the endocarp (known as pit) is the woody structure that surrounds the seed. The kernel of the mango includes the seed inside the fruit, located at the center, and the endocarp (the innermost layer). The endocarp acts as a protective barrier around the kernel, which is hard and inedible Depending on the type of mango, exocarp (7-24%), endocarp (about 6%) and seed (30-45%) of fruit remain as residue, which is often burnt or thrown away. Therefore, cellulose extraction from mango waste are used as alternatives source of cellulose (Choudhary et al., 2023).

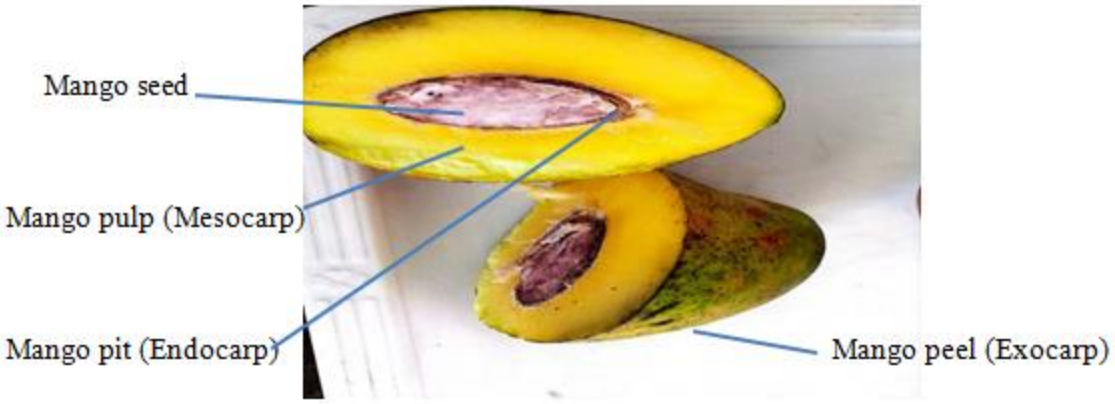

Figure 2: Morphology of mango fruit and its industrial components

1.4. Cellulose isolation methods

Cellulose extraction methods, developed over a long period of time, can be broadly classified into two categories: top-down and bottom-up techniques. Top-down techniques involve isolating cellulose from natural plant biomass by breaking down its complex structure and removing non-cellulosic components like lignin and hemicellulose, leaving behind purified cellulose. In contrast, bottom-up techniques focus on synthesizing cellulose from smaller molecular units, such as glucose or cellobiose, rather than isolating it from plant material. (Trache et al., 2016).

The pretreatment of biomass by different methods removes hemicellulose and lignin from polymer matrix. Pretreatment of lignocellulosic biomass is an intervention process that rapidly disintegrates the lignocelluloses to its primary constituents such as; lignin, cellulose, and hemicellulose. Based on treatment types and their applications, pretreatment processes are mainly categorized into three major categories, including physical (milling, microwave, ultrasound, and pyrolysis),, chemical (acid, alkali, ozonolysis, and organosolvent, ionic liquids), and biological (fungi, bacteria, and archaea) treatments. However, an additional method which is a hybrid of both physical and chemical treatments also exists as physicochemical method (Bhatia et al., 2020).

Physical pretreatment techniques

Physical pretreatment techniques, such as mechanical operations, various forms of irradiation, and ultrasonic treatments, have been employed to improve the accessibility of hydrolysable

polymers within lignocellulosic materials. Among the physical pretreatments, mechanical pretreatment such as chipping, grinding and/or milling is widely used for waste materials, such as agricultural residues or any other crops and forestry residues. The physical pretreatment procedure can increase the lignocellulosic biomass's surface area and pore size while decreasing the cellulose's crystallinity and DP. Depending on the kind of biomass utilized, processing period, and milling method employed, DP and crystallinity can be reduced. The physical pretreatment process is more efficient, simpler, and environmentally friendly technique. Nonetheless, the primary disadvantage of this pretreatment method is its elevated power consumption (Haldar and Purkait, 2021).

Chemical pretreatment techniques

Chemical pretreatment has attracted considerable research interest because of its effectiveness in improving the biodegradation of complex materials. Nonetheless, it has several drawbacks, including the degradation of lignin instead of its separation, rising pH levels during digestion, salt accumulation, corrosive effects from acids, and the generation of process inhibitors. Alkali or acid pretreatment methods are most commonly used pretreatment method with the primary goal of removing lignin and/or hemicellulose. At low pH, the hemicellulose fraction undergoes hydrolysis, whereas the cellulose and lignin fractions are generally less affected. At higher pH, it is instead lignin that is solubilised, which forms the basis for many pulping processes (Norrrahim et al., 2021).

Alkaline pretreatment uses bases like sodium, potassium, calcium, and ammonium hydroxide to treat lignocellulosic biomass. The use of an alkali causes the degradation of ester and glycosidic side chains leading to an increase of internal surface by swelling, a decrease of DP and crystallinity, destruction of links between hemicellulose, cellulose, and lignin and solubilize lignin, hemicellulose and other extractives like pectin. Sodium hydroxide has been thoroughly investigated for many years and has been demonstrated to alter the lignin structure in biomass, thereby improving the accessibility of cellulose to enzymes (Sindhu et al., 2015).

Acid pretreatment can be performed at low temperature with concentrated acid or high temperature with diluted acid to break the rigid structure of the lignocellulosic material. Acid pretreatment with dilute-acid hydrolysis is preferred because concentrated acid are toxic,

corrosive, and hazardous and thus require reactors that are resistant to corrosion which makes the pretreatment process very expensive. The most commonly used acids are sulphuric, hydrochloric, phosphoric, acetic, formic and nitric acids (Zheng et al., 2014).

Biological pretreatment techniques

Although various pretreatment methods are available, biological pretreatment appears particularly promising due to its eco-friendly nature. It avoids the generation of inhibitors and offers the benefit of lower energy consumption. In contrast to physical and chemical pretreatment methods, biological pretreatment generally demands less energy, does not produce toxic compounds, avoids the use of chemicals, and yields a high amount of desired products. Additionally, it is performed under milder conditions, resulting in minimal generation of inhibitors that could adversely impact anaerobic digestion. The foremost limitations in using this strategy is long incubation time for effective delignification (Sindhu et al., 2016).

Physicochemical pretreatment techniques

Physicochemical pretreatment is one of the most successful pretreatment methods. Steam explosion (SE), also known as auto-hydrolysis is one example of physicochemical pretreatment involves exposing lignocellulosic material to a high temperature and high-pressure saturated steam for a few minutes. The heating temperature causes a catalytic reaction that breaks down the hemicellulose and changes the lignin content, preparing the substrate for hydrolysis. Variables including moisture content, particle size, residence duration, and temperature can all affect effectiveness of SE (Karimi et al., 2013).

Delignification and bleaching

Delignification is the next step that focuses on removing lignin, a complex and rigid polymer that binds cellulose fibers in plant cell walls. By breaking down and removing lignin, delignification enhances the accessibility of cellulose for further processing. This process is typically achieved through chemical treatments, such as alkaline treatments and acidic treatments**.** After delignification, a post-pretreatment process called bleaching is applied to further purify the cellulose by removing any residual lignin, hemicellulose, and other color-imparting impurities. Its goal is to increase their brightness by chemical means. Chemicals like a

combination of sodium hypochlorite and glacial acetic acid or hydrogen peroxide and sodium hydroxide can be used as bleaching agents. Nowadays, there is increasing interest in using hydrogen peroxide as one of the oxidants to replace chlorine-based reagents due to the introduction of completely chlorine-free bleaching methods (ARNATA et al., 2019)

1.5. Modification of cellulose

Although cellulose in its polymeric form is an excellent material for the manufacturing of many useful products, often it does present limitation for different pharmaceutical applications. The physical properties of cellulose, such as its high water absorption capacity, poor strength, limited heat stability and tendency to form aggregates, can affect their use in pharmaceutical formulations. In order to use cellulose in these areas and to improve its intrinsic value, modification is crucial (Shokri and Adibkia, 2013).

Modified cellulose derivatives often exhibit enhanced properties such as increased strength, flexibility, stability, water resistance, or biodegradability compared to native cellulose. Chemically modified polymers have been extensively investigated in order to develop new biomaterials with innovating physicochemical properties. Different derivatives have been formed to enhance these physicochemical characteristics of cellulose. A common modification technique involves hydrolyzing amorphous cellulose with mineral acids to produce MCC, which is a highly crystalline powder with finer particle sizes. Modified polymers, including cellulose ethers like hydroxypropylmethylcellulose, hydroxyethylcellulose, and carboxymethylcellulose, are important classes of modified cellulose (Nasatto et al., 2015).

Cellulose modification methods such as chemical modification (esterification, acylation, etherification), physical modification (milling/ grinding, granulation) and enzymatic modifications (cellulase treatment, hydrolysis) are used to produce a wide range of cellulose derivatives (Tkacheva et al., 2013).

Physical modification

Physical modification of cellulose involves altering its structure or properties without changing its chemical composition. This can be achieved through various processes, such as mechanical treatment, heat application, or the use of ultrasound or radiation. Mechanical treatment, like grinding or milling, breaks down cellulose into smaller particles, increasing its surface area and

enhancing its reactivity. Heat treatment can be used to change the crystallinity of cellulose, making it more flexible or improving its water absorbency. The application of ultrasound or irradiation can also disrupt the cellulose structure, leading to changes in its solubility and reactivity. These physical modifications allow cellulose to be more easily processed and utilized in a variety of applications, including (Aziz et al., 2022).

Chemical modification

Chemical modification of cellulose involves altering its molecular structure by introducing new functional groups or changing existing ones, thereby enhancing its properties and expanding its range of applications. The building blocks of cellulose, the AGU contain repeating OH groups which are highly reactive and can be modified by interacting with different functional groups and yielding a diverse array of cellulose derivatives. One common chemical modification method is etherification, where alkyl or aryl groups are added to cellulose, making it more soluble in water or organic solvents. This includes the production of derivatives like hydroxyethyl cellulose and ethyl cellulose, which are widely used in pharmaceutical industries. Esterification is another chemical modification method, where cellulose is reacted with acids like acetic acid, results in compounds like cellulose acetate, which is soluble in organic solvents and used as pharmaceutical coating excipients. Another approach is carboxymethylation, which introduces carboxymethyl groups to cellulose, making it more water-soluble and useful as a thickening agent, stabilizer, or emulsifier pharmaceutical and food products. Oxidation is also a common chemical modification, which partially breaks down the cellulose structure, increasing its reactivity and providing new functionalities, such as enhanced water retention or better bonding properties. Chemical modification opens up new possibilities for cellulose, enabling it to be utilized in a variety of pharmaceutical products (Hon, 2017).

Enzymatic modification

Enzymatic modification of cellulose involves the use of specific enzymes to alter the cellulose structure, it offers a more environmentally friendly approach compared to chemical methods. One of the most common enzymes used in this process is cellulase, which breaks down cellulose into smaller units. Enzymatic modification is used in the pharmaceutical and food industries to produce cellulose derivatives that serve as thickening agents, stabilizers, or controlled-release excipients. This method offers several advantages, including milder reaction conditions and

fewer by-products, making it a sustainable and effective way to modify cellulose for a wide range of applications (Martinelli et al., 2021).

1.6. Microcrystalline cellulose

MCC is partially depolymerized cellulose prepared by treating cellulose obtained as a pulp from fibrous plant material with mineral acids. MCC is defined by DP less than 350 glucose units, compared to DPs in the order of 10,000 units for the original native cellulose . The microcrystals in natural cellulose are packed side by side tightly in the fiber direction, joined by amorphous hinges, in a compact structure resembling bundles of wooden matchsticks. The amorphous hinge is readily hydrolyzed when subjected to acid hydrolysis. This results in shorter and more crystalline fragments (as shown in Figure 3). As a result, the DP of the cellulose chain decreases with almost no loss in weight. MCC occurs as a fine white, odorless, crystalline powder, which is insoluble in water, dilute acids and alkali and common organic solvents. There are noticeable differences in the chemical composition, morphology, crystallinity, surface area, moisture content, porous structure, and DPof MCC derived from diverse sources (Chaerunisaa et al., 2019).

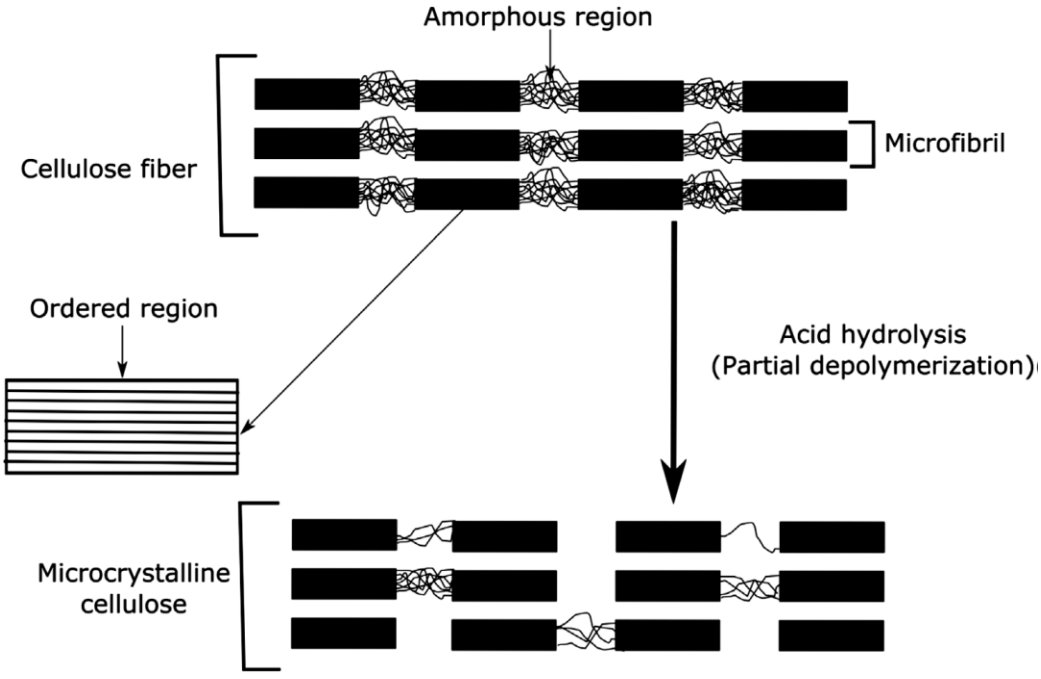

Figure 3: Schematic diagram of MCC separation during acid hydrolysis (Trache et al., 2016)

1.7. Pharmaceutical Application of cellulose and Microcrystalline cellulose

Cellulose is widely used in a variety of commercial applications in pharmaceutical industries due to its high availability and attractive chemical and physical properties such as biocompatibility, biodegradability, thermal and chemical stability. The production of cellulose derivatives broadens the applications of cellulose by modifying the polymer chemically or physically in terms of hydrophobicity, processability and solubility. For application as excipient in pharmaceutical industry, an important aspect is the improvement in processability of cellulose; in this sense, the most important cellulose derivative is MCC (Aziz et al., 2022).

The MCC is an important ingredient in pharmaceutical (as binders, adsorbents, flowability enhancer), food (as stabilizers, anti-caking agents, fat substitutes and emulsifiers), beverage (as gelling agents, stabilizers, anti-caking agents and suspending agents), and cosmetic (as fat substitutes, thickeners, binders). In solid dosage form, it is employed as filler-binder in tablet formulations to enhance compactibility. MCC is a common excipient that can function as both a filler (providing bulk) and a binder (enhancing tablet cohesion). Moreover, it's regarded as one of the best excipient' the best excipient for direct compression (DC) tableting and it is one of the mostly used filler-binders in direct tablet compression. DC tableting is the most economical technique in the production of large number of tablets. MCC popularity in DC is due to its excellent binding properties when used as a dry binder. MCC possesses almost ideal properties as it is highly compressible with maximum dilution potential, self-lubricating, glidant and disintegrant (Chaerunisaa et al., 2019).

The hydroxyl groups (-OH) present on MCC facilitate the formation of hydrogen bonds with neighboring MCC particles and other substance, which strengthens particle cohesion and enhances the hardness and stability of tablets. Additionally, the irregular shape and rough surface of MCC increase its surface area and provide numerous contact points for particle bonding. This surface texture and irregularity aid in interlocking the particles, resulting in strong binding within the tablet structure. In contrast, MCC with a lower degree of crystallinity often has a more porous structure and tends to exhibit higher water uptake and swelling capacity. This porous structure enhances water diffusion into the particles, facilitating faster and more efficient disintegration of the dosage form(Saigal et al., 2009, Chaerunisaa et al., 2019).

MCC has been used successfully for DC with many drugs. In addition to its use in DC formulations, MCC is used as a diluent in tablets prepared by wet granulation as well as a filler for capsules. In its colloidal form, MCC is used as a suspension stabilizer, water retainer, viscosity regulator, and emulsifier in various pastes and creams. Features like high mechanical strength and stiffness combined with renewability, biodegradability, non-toxicity, large surface area, low density, biocompatibility, water insolubility, crystallinity make MCC more attractive to be used in various industrial fields. However, MCC suffers some drawbacks that are desired for some applications such as poor wettability, moisture absorption, incompatibility with most polymeric matrices and limitation in processing temperature (Zhao et al., 2022).

1.8. Statement of the Problem

The pharmaceutical industry relies heavily on excipients, which are essential components of drugformulations, serving as binders, disintegrants, fillers, and stabilizers. Among these MCC is one of the most widely used directly compressible excipients due to its exceptional binding capacity, compressibility, and disintegration properties. However, the primary source of MCC, wood pulp, raises significant environmental concerns, including deforestation, habitat destruction, and the depletion of natural resources, which are critical issues in the context of global climate change and biodiversity loss (Trache et al., 2016).

In recent years, there has been growing interest in exploring agricultural by-products as sustainable and eco-friendly sources of cellulose for MCC production. Agricultural wastes, such as fruit peels, seeds, and kernels, are abundant, renewable, and often underutilized, making them attractive candidates for the extraction of cellulose. According to the FAO (2023), mango is one of the most widely cultivated fruits in tropical and subtropical regions, with worldwide production over 55 million metric tons each year. Mango processing generates substantial quantities of kernels as by-products, which account for 15-20% of the total fruit weight. This results in an estimated global production of 8 to 11 million metric tons of mango kernels annually. These kernels are rich in cellulose, making them a potential raw material for the isolation of MCC. However, despite their high cellulose content and availability, mango kernels remain largely unexplored as a source of MCC for pharmaceutical applications (Ganeshan et al., 2016).

Large-scale disposal of mango waste after fruit processing, leading to environmental pollution and resource underutilization. This issue is more common in developing countries, where a significant amount of these residues are either burned or discarded into rivers. Burning agricultural residues can release dangerous pollutants into the air, while improper disposal can lead to contamination of water sources, impacting both ecosystems and human health (Donner et al., 2020).

Pharmaceutical manufacturing companies in Ethiopia import pharmaceutical excipients (including MCC) from abroad. This requires a significant amount of foreign currency, potentially imposing a substantial burden on the country's economic development. Failure to efficiently utilize agricultural by-products results in missed opportunities to generate economic value. Furthermore, agricultural wastes are abundant and accessible, and the process involved in the production of MCC is simple and economical. The scarcity of cotton and wood in various regions has led to increased interest in non-wood materials such as aquatic plants, grasses, agricultural residues, and their by-products. These alternatives are considered valuable sources of cellulosic fibers because they are abundantly locally available and renewable. This study was aimed at investigating Mango kernel fiber as potential source of cellulose and MCC and evaluation of MCC as direct compressible excipient (Donner et al., 2020).

1.9. Significance of the Study

The conversion of mango kernel (MK) waste to MCC has the potential to decrease deforestation, conserve natural resources, prevent polution and promote sustainable resource management by lowering the demand for woody plant materials. The study provides a sustainable solution to the increasing demand for eco-friendly and cost-effective excipients by utilizing mango kernels. It aligns with the principles of a circular economy by transforming waste into a valuable resource and reducing environmental pollution. Currently, the pharmaceutical industry depends heavily on wood and cotton for MCC production, which are resource-intensive. The study addresses the need for diversification in excipient sources. This study also help to create an additional income stream for farmers, especially in regions where mango cultivation is a significant agricultural activity (Sarkis et al., 2010).

The study has significant economic implications. preparing MCC from mango kernels can lower the cost of pharmaceutical formulations, making medicines more affordable, especially in developing countries where healthcare costs are a major burden. This aligns with global efforts to improve access to affordable healthcare and supports Sustainable Development Goal. The worldwide MCC market was valued at 1.140 Billion USD in 2022, and by 2031, it is expected to grow to 2.04466 Billion USD. Non-wood sources, which has a lower overall production cost and a more competitive selling price, are considered as potential sources to satisfy this worldwide need for MCC (Tessema et al., 2023).

The results of this study can provide insight into the properties of the cellulose found in mango kernels and their modified derivatives (MCC). Moreover, further projects can be designed to fulfill the cellulose demand of the country for other sectors like food, textile and paper industries. The results of this study can be also used as a recent source of information for those who need to conduct further investigations in this area.

2. OBJECTIVES

2.1. General Objective

- ✓ To characterize and evaluate MCC isolated from mango kernel as a direct compressible pharmaceutical excipient in tablet formulation

2.2. Specific Objectives

- ✓ To extract cellulose from mango kernel
- ✓ To prepare MCC from mango kernel cellulose
- ✓ To characterize the native cellulose and the resulting MCC
- ✓ To evaluate the resulting MCC as a directly compressible pharmaceutical excipient

3. MATERIALS AND METHODS

3.1. Materials

Mango kernels collected from Maksegnit local farm near Gondar (2,600 meters above sea level, 12.5° N). Species identification of mango were conducted at the Department of Biology, University of Gondar by Dr. Daniel Tadesse. The results confirmed that the species was Mangifera indica (DT01/2024). Paracetamol powder was kindly donated by Ethiopian Pharmaceuticals Manufacturing Share Company (EPHARM). Acetic acid 99.8% (PENTOKEY ORGANY, India), Formic acid 98% (PENTOKEY ORGANY, India), Xylene 98% extra pure (Himedia Laboratories, India) and Hydrogen peroxide 30% (Farmatalia Carlo erba reagents S.P.A. Italy) purchased from Nigat Chemicals Trading. Ammonia solution 28% (Farmatalia Carlo erba reagents S.P.A. Italy), Cupric sulphate pentahydrate 98.5% (Himedia Laboratories, India) , Sulphuric acid (Labmerk,India), Potassium iodide (Blulux, India), Silica gel (Labmerk,India), Diethyl ether (Central Drug House Ltd, India), Ethanol 96% (Blulux laboratory Ltd, India) , Sodium chloride 99.8% (Blulux, India), Hydrochloric acid 37% (BDH chemicals ltd, England), Iodine (Avishkar international, India), Sodium hydroxide 99.8% (Blulux, India), and Toluene 99.5% (Blulux, India) were received from University of Gondar pharamaceutics, pharmaceutical chemistry and organic chemistry laboratories. Zinc chloride (Loba Chemie Pvt. Ltd., India) from Bahir Dar university, Magnesium stearate (Bulvinos Chemicals Ltd, England) and Avicel PH-101 from Addis Ababa University were used as received. All chemicals and reagents were analytical grade.

3.2. Methods

3.2.1. Extraction of Cellulose from mango kernel

The edible part of the mango (mesocarp) was removed and thoroughly washed with water. Mango kernels were dried properly at 40 ^{o}C in the oven for 24 hours. The dry mango kernels were crushedusing hammer mill screened using a sieve (2 mm). The resulting mango kernel powder was then dewaxed with toluene and ethanol (2:1) for 6 h in a soxhlet apparatus (Nwadiogb et al., 2015). The dewaxed mango fiber was boiled in 10% (w/v) NaOH solution in 1:10 solid to liquid ratio on a water bath at 90^{o}C for one and half hour by covering the flask with

aluminum foil. After filtering through nylon cloth, the mango residue was washed with distilled water repeatedly until it become whitish and further delignified with a mixture of 20% formic acid (FA)/20% acetic acid (AA)/7.5% H_2O_2 (2:1:2) solution with 1:10 (w/v) solid to liquid ratio of dry material in water bath for 90 min at 90°C . Following filtration and washing with distilled water, the residue was bleached with 7.5% H_2O_2 in alkaline media of 4 % NaOH solution at 1:10 fiber ratio, first at room temperature for 30 min then on water bath at 70 °C for 30 min. Finally, it was repeatedly washed with distilled water until its pH(BANTE Instrument CO. ltd, China) becomes neutral, filtered by nylon cloth and oven-dried (WH-71, China) at 60°C to constant weight (Gabriel et al., 2020).

3.2.2. Microcrystalline cellulose preparation

Using the method described by Battista (1950) with some modification, the cellulose was hydrolyzed to produce MCC. 2.5M of HCl was heated to temperature of 100 ^{o}C on hotplate. The cellulose that was isolated from the mango kernel was added into boiling acid (1:20 fiber-to-liquor ratio) and allowed to boil for 30 minutes at 105°C with constantly stirring (125 rpm). After completion of the boiling time, the prepared mango kernel MCC was filtered using nylon cloth and washed with distilled water followed by 5% ammonium hydroxide solution. It was then washed repeatedly with distilled water till the filtrate have neutral pH. The resulting MCC was dried using a Tall Form Spray Drier (FT80, England) at 16% consistency (w/v) air pressure of 1 bar and at inlet and outlet temperature of 175 °C 120 °C respectively. Finally, it was ground using glass mortar and pestle and screened via 224 μm sieve.

3.2.3. Determination of percent yield

The following equation was used to calculate the yield of cellulose (Eq 1) and MCC (Eq 2) based on the dry weight of mango kernel.

$$\text{Cellulose } \% = \frac{\text{weight of dry cellulose residue(g)}}{\text{weight of original fiber sample (g)}} \times 100 \ldots\ldots\ldots\ldots\ldots\ldots\ldots\ldots\ldots\ldots\ldots\ldots\ldots\ldots \text{Eq 1}$$

The formula below was used to determine the yield of MCC

$$\text{MCC \%} = \frac{\text{weight of prepared MCC(g)}}{\text{weight of prepared Cellulose(g)}} \times 100 \ldots\ldots\ldots\ldots\ldots\ldots\ldots\ldots\ldots\ldots\ldots\ldots\ldots\ldots \text{Eq 2}$$

The average of three separate determinations was used to express the results.

3.2.4. Characterization of microcrystalline cellulose

In this study, SEM, FTIR, XRD, and TGA/DTG were used to characterize both cellulose and MCC, while others were applied exclusively to MK-MCC powders. Commercial MCC (Avicel PH-101) was used as a standard for comparing its properties.

3.2.4.1. Chemical identification test

Zinc chloride solution that has been iodinated was used for the identification test. Iodinated zinc chloride was prepared by dissolving 6.5 grams of potassium iodide and 20 grams of zinc chloride in 10.5 milliliters of distilled water. It was then shaken for 15 minutes after addition of 0.5 gram of iodine. 10 mg MK-MCC powder was placed on a petri dish and dispersed in 2 ml of iodinated zinc chloride solution and the resulting color is observed (USP, 2007).

3.2.4.2. Degree of polymerization

The degree of polymerization (DP) refers to the average number of glucose units linked together in a macromolecule or polymer such as cellulose or its derivative molecule. Cupper-ammonium hydroxide (Cuam) solution was used as a solvent to determine the DP of cellulose and MCC made from mango kernel. Freshly precipitated $Cu(OH)_2$ was dissolved in aqueous ammonia to prepare the Cuam solution. Initially, 600 ml of distilled water was used to dissolve 28 g of cupric sulphate pentahydrate and filtered into a beaker. By adding 14 milliliters of 25% aqueous ammonia, Cu(OH)2 was precipitated. It was then filtered and repeatedly washed with distilled water until it become sulfate free . Then cuam solution was formed by dissolving the precipitate with 500 ml NH_4OH (25%).

100 mg of each sample was dissolved in the 100 ml of Cuam solution by vigorously shaking the mixture and then placed in water bath at 25^{o}C for 5 min. After the sample was completely dissolved in cuam solvent, the sample solution was transferred to Ostwald Capillary viscometer

(BDH, England) and viscosity measurement was carried out (Liebert and Klemm, 1998). DP was calculated from following equation

$$\mathrm{DP} = \frac{2000 \times \eta\mathrm{spec}}{\mathrm{c\ x\ }(1 + 0.29\mathrm{\ x\ }\eta\mathrm{spec})} \ldots\ldots\ldots\ldots\ldots\ldots\ldots\ldots\ldots\ldots\ldots\ldots\ldots\ldots\ldots\ldots\ldots\ldots\ldots\ldots\ldots Eq\ 3$$

$$\eta\mathrm{spec} = (\frac{\mathrm{t}}{\mathrm{to)}}\text{-1}) \ldots\ldots\ldots\ldots\ldots\ldots\ldots\ldots\ldots\ldots\ldots\ldots\ldots\ldots\ldots\ldots\ldots\ldots\ldots\ldots\ldots\ldots\mathrm{Eq\ 4}$$

Where ηspec is specific viscosity; η $\eta 0$ is relative viscosity; c is concentration in g/l; *t*, is the time required (in seconds) for the sample to travel from upper graduated mark to the lower graduated mark and t_0, the time required for pure solvent to travel from upper graduated mark to the lower graduated mark. The molecular weight of cellulose and MCC samples were determined from DP by using Eq 5. The determination was performed in triplicate

$$\text{Molecular wieght } = \mathrm{DP\ X\ 162} \ldots\ldots\ldots\ldots\ldots\ldots\ldots\ldots\ldots \mathrm{Eq\ 5}$$

3.2.4.3. Determination of Water soluble substances

Conical flask containing the mixture of 2g MCC powder and 32 ml of distilled water was shaken for 10 min. After being filtered using filter paper the mixture was transferred to a beaker and evaporated on hot plate at 105 °C for 1 hour dryness without charring and weighed. The amount of water soluble substance was the difference between the weight of beaker along with residue and the weight of empty beaker. The experiment was performed in triplicates and the average of three determinations taken (USP, 2007).

3.2.4.3. Determination of ether-soluble Substances

Ten grams of MCC powder was placed in column chromatography developed using silica gel and ether to which 50 ml of peroxide-free ether was passed. Secondly, same amount blank solvent (ether) was eluted through similarly developed column. After both eluates were evaporated to dryness to constant weight the dried residue was cooled in a desiccator and weighted. The procedures were done three times and the difference between average of three experiment of blank and sample eluate residues was taken as the amount of ether-soluble matter in the sample (USP, 2007).

3.2.4.4. Ash value determination

Crucible was first cleaned, oven dried at 100 °C for 30 min and then cooled in desiccator containing silica gel for 30 min. Three gram MCC powder was placed on the crucible and heated till the smoking was stopped. The residue was charred in furnace at 550 °C for 2 h then cooled in desiccator for 45–60 min. Ash value was calculated as weight percentage of the ratio of charred residue and MCC sample (Kambli et al., 2017).

3.2.4.5. pH determination

One gram of MCC powder were manually shaken with 50 mL of distilled water for 5 minutes. After allowing the mixture to settle, the pH of the resulting supernatant liquid was measured using a pH meter (BANTE Instrument CO. ltd, China) (Kambli et al., 2017).

3.2.4.6. Hydration capacity

One gram of each sample was placed into four 15 ml plastic centrifuge tubes. Subsequently, 10 ml of distilled water was added to each tube, and the tubes were sealed. The content were vigorously shaken manually for 20 min with 5 min intervals. The mixture was centrifuged at 2000 rotations per minute (rpm) for 15 min. After decanting the supernatant, the centrifuge tubes were stoppered and weighed. The hydration capacity (HC) was expressed as a ratio of gain in weight after hydration to the weight of the dry sample (Gbenga and Fatimah, 2014).

$$\text{Hydration Capacity} = \frac{\text{ws}}{\text{wd}} \quad \text{Eq 14}$$

Where, Ws and Wd are weights of the centrifuge tube with sediment and dry sample, respectively

3.2.4.7. Moisture content

Three gram of MCC placed on a pre-weighed Petri dish, and the dish was heated at 105°C in an oven for 2 hours. After drying MCC until it had a constant weight by checking it every 30 minutes, the weight of the MCC was measured. Triplicate studies were done and moisture content was calculated as follows (Trache et al., 2014).

$$\text{loss on drying (\%)} = \frac{\text{Mass loss on heating(g)}}{\text{Weight Sample used (g)}} \times 100 \ldots\ldots\ldots\ldots\ldots\ldots\ldots\ldots\ldots \text{Eq } 6$$

3.2.4.8. Moisture sorption pattern

The powders of MK-MCC was dried in an oven for 4 h at 105 ^{o}C. Then 1 gm powder was distributed evenly on a pre-weighed petri plate and placed in desiccators containing distilled water (100% RH), saturated solution of NaCl and appropriate concentrations of NaOH, i.e., 24.66%, 31.58% and 40% of NaOH solutions to provide 60%, 40% and 20% RH, respectively and stored at 25^{o}C. Samples were equilibrated for 4 weeks at room temperature. After four weeks, the weights were noted, and the weight difference between the samples' pre- and post-equilibration weights in a particular RH chamber was used to determine each sample's moisture absorption. Water sorption capacities of the samples were expressed as percent moisture uptake. Results were expressed as a mean of three parallel determinations

$$Moisture\ sorption\ capacity = \frac{W2-W1}{W1} * 100 \ldots\ldots\ldots\ldots\ldots\ldots\ldots\ldots\ldots\ldots\ldots\ldots\ldots\ldots\ldots\ldots\ldots Eq\ 15$$

Where W1 is the weight of the sample before exposure and W2 is the weight of the sample after exposure (Heng et al., 2004).

3.2.4.9.Fourier transform infrared spectroscopy (FTIR)

Five mg of the sample was mixed with 5ml liquid paraffin and coated on KBr plate rinsed with alcohol. After spreading the sample mixture on one potassium bromide (KBr) plate, the other KBr plate was placed on top of the first plate. The sandwiched samples were inserted into the infrared spectrometer, and the spectra were recorded.. FTIR spectroscopy (FTIR650, Biobase, China) was also used to analyze the paracetamol and MK-MCC compatibility investigation. The FTIR spectra of paracetamol powder alone and its physical mixture with the prepared MCC powder (1:1) were recorded at 4000-400 cm^{-1} using FTIR650,

3.2.4.10. Morphological characterization

Scanning electron were used to study morphologies of cellulose and MCC. The scanning electron micrographs were taken at an accelerating voltage of 20 KV and the samples were then viewed and photographed.

3.2.4.11. X-ray diffraction (XRD)

The crystalline structure of cellulose and MCC from mango kernel were analyzed by X-ray diffractometer (SHIMADZU Corporation, Japan) at 40 KV. The Percentage crystallinity index (CrI %) was calculated using the following formula.

$$Crl = \frac{(I002 - Iam)}{I002} \times 100 \ldots\ldots\ldots\ldots\ldots\ldots\ldots\ldots\ldots\ldots\ldots\ldots\ldots\ldots eq\ 7$$

Where I_{002} represents crystalline material and I_{am} represents the amorphous material

3.2.4.12. Thermal analysis (TGA)

A thermogravimetric (TGA)/differential thermal analysis (DTA) apparatus (SHIMADZU corporation, Japan) was used to perform thermal stability analysis.10 mg of each samples were heated from room temperature to 800 ^{o}C with a scanning rate of 20 ^{o}C/min under a nitrogen atmosphere. The weight percentage of residue was recorded to determine the weight losses of the sample after heating (Das et al., 2010).

3.2.4.13. Particle size analysis

Particle size analysis was conducted using the Malvern Mastersizer 2000 laser diffraction particle size analyzer (Malvern Instruments Ltd, Worcestershire, WR14 1XZ, UK). Approximately 500 mL of distilled water was used to immerse the sampling port of the Hydro dispersion unit. A background reading was taken with this dispersing medium (distilled water). Next, 92.5 mg of MCC powder was dispersed to the distilled water until an obscuration level of 15-20% was achieved, which measures the amount of laser light lost due to the presence of the sample in the analyzer beam. The software (Mastersizer 2002) was used to determine the mean volume particle size distribution, mean particle size, specific surface area, and percentile distribution of the samples. The analysis was conducted under the following conditions: the size range was set from 0.05 to 900 μm with a 300 RF, the active beam length was 2.4 mm, and the MS1 Small Volume Sample Dispersion Unit was used. The dispersion mode was polydisperse, the standard was set to wet, and the presentation type was 3OHD. The measurements were performed in triplicate, and the results were averaged along with their corresponding standard deviations (Lee et al., 2019).

3.2.4.14. Density and related properties

Bulk Density and tapped Density

A 50 mL dry and clean measuring cylinder was filled with 10 grams of MCC powder (m) and volume occupied by the powder was recorded (Vb). The volume occupied after the measuring cylinder was tapped about 300 times on a soft surface bench was determined and recorded as Vt. To make sure the data was reliable, the average value of three independent determinations was finally taken and the average volume was determined and recorded. The bulk and tap densities were determined using the following equations (Adeleye et al., 2022).

$$\text{Bulk Density} = \frac{\text{m}}{\text{Vb}} \ldots \ldots \ldots \ldots \ldots \ldots \ldots \ldots \ldots \ldots \ldots \ldots \ldots \ldots \ldots \ldots \ldots \ldots \ldots \ldots \ldots \ldots \ldots \ldots \ldots Eq\ 8$$

$$\text{Tapped Density} = \frac{\text{m}}{\text{Vt}} \ldots \ldots \ldots \ldots \ldots \ldots \ldots \ldots \ldots \ldots \ldots \ldots \ldots \ldots \ldots \ldots \ldots \ldots \ldots \ldots \ldots \ldots \ldots \ldots \ldots Eq\ 9$$

Carr's Index and Hausner Ratio

Carr's index and Hausner ratio were calculated by using the following equations:

$$Carr's\ Index = \frac{(Bulk\ volume\ -\ Tapped\ volume)}{Bulk\ volume} \times 100 \ldots \ldots \ldots \ldots \ldots \ldots \ldots \ldots \ldots \ldots \ldots \ldots Eq\ 10$$

$$Hausner\ Ratio = \frac{Bulk\ Volume}{Tapped\ Volume} \ldots \ldots \ldots \ldots \ldots \ldots \ldots \ldots \ldots \ldots \ldots \ldots \ldots \ldots \ldots \ldots \ldots \ldots \ldots \ldots \ldots \ldots Eq\ 11$$

True Density

True density was determined using the liquid displacement method with xylene as the immersion fluid. Initially, 25 mL of xylene was added to a pre-weighed empty pycnometer, which was then sealed and re-weighed. After draining out the xylene, 2 grams of MCC sample were introduced into the pycnometer, and xylene was added to fill it. The mixture was stirred for 10 minutes with a glass stirrer to eliminate trapped air, stopping once no more air bubbles were visible in the xylene. The sample was allowed to settle, and the volume was adjusted to 25 mL with additional xylene. The true density (g/mL) was finally determined with the following calculation.

$$\text{True density} = \frac{\text{W1} \times \text{SG}}{[(\text{W1} + \text{W2}) - \text{W3}]} \ldots \ldots \ldots \ldots \ldots \ldots \ldots \ldots \ldots \ldots \ldots \ldots \ldots \ldots \ldots \ldots \ldots \ldots \ldots \ldots \ldots \ldots Eq\ 12$$

Where, W1 = weight (g) of sample, W2 = weight (g) of the pycnometer filled with xylene, W3 = weight (g) of pycnometer with sample plus xylene, and SG = specific gravity of xylene (g/mL) which is determined from weights of empty pycnometer and pycnometer filled with xylene

Porosity

The porosity of MCC powders was calculated using the formula stated by Kambli *et al*., 2017

$$\varepsilon = \left[1 - \frac{(\rho bulk\ )}{(\rho true)}\right] * 100 \ldots \ldots \ldots \ldots \ldots \ldots \ldots \ldots \ldots \ldots \ldots \ldots \ldots \ldots \ldots \ldots \ldots \ldots \ldots \ldots \ldots \ldots \ldots \ldots \ldots Eq\ 13$$

Where ρbulk is the bulk density, ρtrue is the true density and ε is the porosity.

3.2.5. Tablet compresion

To study the compressibility and compactibility of MK-MCC and Avicel PH 101 plain tablets, the respective powders were compressed at different compression forces (CF). Plain tablets were compressed at 50N (CF1), 75N (CF2), 100N (CF3), 125N (CF4), and 150N (CF5) with 11mm diameter tablet machine (EC0 Press, 7891, India). MK-MCC powder (400 mg) and Avicel PH 101 (400 mg) were filled into the die before each compression. Tablet property evaluations were conducted for both plain MK-MCC and Avicel PH101 across the CF1 to CF5 formulations.

3.2.5.1. Dilution potential

To evaluate dilution potential, MK-MCC powders were compressed with paracetamol at concentrations of 35%, 50%, 65%, and 80% under a constant compression force of 100N, using flat punches with an 11 mm diameter. Before compression, paracetamol and MK-MCC powders were mixed for 10 minutes in a Turbula mixer set at 45 rpm. Tablet property evaluations were conducted on both plain MK-MCC and Avicel PH101 at different concentrations of paracetamol (35%, 50%, 65%, and 80%).

3.2.5.2. Lubricant sensitivity test

The lubricant sensitivity test (LST) was performed on tablets weighing 400 mg, which contained either plain MK-MCC powder or MK-MCC with 0.5% magnesium stearate. These tablets were compressed at 100N to evaluate the lubricant sensitivity of MK-MCC. Lubricant sensitivity was quantified using the lubricant sensitivity ratio (LSR).

$$LSR = \frac{So - Slub}{So} \ldots\ldots\ldots\ldots\ldots\ldots\ldots\ldots\ldots\ldots\ldots\ldots\ldots\ldots\ldots\ldots\ldots\ldots\ldots\ldots\ldots\ldots\ldots\ldots\ldots\ldots \text{Eq } 17$$

So is compact crushing strength without lubricant, and Slub is compact crushing strength with added lubricant (Getachew et al., 2023).

3.2.6. Evaluation of tablet

Before the evaluation of the tablets for their crushing strength, tensile strengths, friability, disintegration time and dissolution, tablets was given a 24-hour post-compression period.

3.2.6.1. Weight and thickness

Twenty tablets were randomly selected and weighed individually with an analytical balance to compute the average weight and standard deviation. The diameter and thickness of the tablets were measured using a hardness tester (Pharma Test, Germany).

3.2.6.2. Crushing strengths and Tensile strength

A hardness tester (Pharma Test, Germany) was used to measure the crushing strength of each of randomly selected ten tablets from each formulation after 24 hours production.

The equation below was used to calculate the radial tensile strength using the crushing strength, tablet diameter, and tablet thickness.

$$\sigma x = \frac{2F}{\pi DT} \ldots\ldots\ldots\ldots\ldots\ldots\ldots\ldots\ldots\ldots\ldots\ldots\ldots\ldots\ldots\ldots\ldots\ldots\ldots\ldots\ldots\ldots\ldots\ldots\ldots\ldots \text{Eq } 16$$

Where σx is the tensile strength, F is the crushing strength, D is the diameter of the tablet, and T is the tablet thickness.

3.2.6.3. Friability test

The weight of ten randomly selected tablets were determined collectively on an electronic balance. The tablets were then placed in the drum of a Friability tester (Pharma Test, Germany) revolving at 25 rpm for 4 min. The tablets were subsequently dedusted and weighed, and the percentage of weight loss was calculated to determine their friability

3.2.6.4. Disintegration time test

Six randomly selected tablets were placed in the tube of USP disintegration test apparatus (Pharma Test, Germany). The assembly was suspended in the beaker with 900 ml distilled water as medium at 37 ± 2ºC at 50 rpm. The time taken for each compact to completely break up and pass through the mesh was noted.

3.2.6.5. Construction of calibration curve

A stock solution of paracetamol with a concentration of 200 µg/mL was prepared using a phosphate buffer at pH 5.8 as the dissolution medium. From this stock solution, seven different concentrations (5.5, 7, 8.5, 10, 11.5, 13, and 14.5 µg/mL) were prepared and their UV absorbances were measured at 243 nm with UV/Visible spectrophotometer (Aginet Technologies, USA) using phosphate buffer (pH 5.8) as a blank (USP, 2007). The plot of absorbance against concentration was plotted, and a linear regression equation and correlation coefficient were derived

3.2.6.6. *In-vitro* drug dissolution test

The dissolution test was done according to the USP specification using dissolution apparatus Type II with 900 ml phosphate buffer (pH 5.8) as the dissolution medium at 37 ± 0.5ºC and 50 rpm. Five ml aliquots of the dissolution medium were removed at 5, 10, 15, 20, 30, 45 and 60 min and filtered using filter paper. Equal amount of fresh medium kept at the same temperature was added into the dissolution vessel to maintain a sink condition. 1 ml of the filtered samples was diluted to 25 ml and absorbance readings were taken with a UV/Visible spectrophotometer at 243nm using phosphate buffer (pH 5.8) as a blank.

3.2.6.7. Statistical analysis

The results were analyzed using independent sample t test and Analysis of Variance (ANOVA) with a statistical software Origin 2024 (OriginLab™ Corporation, USA) and SPSS. At a 95% confidence level, p values less than or equal to 0.05 were considered statistically significant.

4. RESULTS AND DISCUSSION

4.1. Identification Test, Organoleptic Properties and Yield of MCC

The experimental findings of the identification test showed that in an iodinated zinc chloride solution, the color of both isolated MK-cellulose and MK-MCC changed to violet-blue. According to USP 30/NF 25 specifications, the violet-blue colour indicates the presence of cellulose/MCC.

The yield of cellulose isolated from mango kernels was found to be 36.50% (±1.57). This yield was higher than the cellulose yields reported in previous studies for orange peel (20.46%) and mango kernels (25.2%) (Ng, 2019, Nwadiogb et al., 2015). However, it was lower than the yields from sugarcane bagasse (40.59%) and walnut shells (42.36%). This yield diference could be resultrd from extraction and source variability (Harini and Mohan, 2020).

The yield of MK-MCC was 78.46% (±1.34) from isolated mango kernel cellulose and 28.64% from raw material. It was higher when compared to the yield of other sources such as raw cotton cochlospermum planchonii (21%), orange peels (8.50%), rice husk (25.05%) and date seeds (12.51%) on the basis of their respective raw materials. However yield of MK-MCC was less than the yield from jute fibres (48-52.8%). This discrepancy could result from the difference of methods and chemicals used in extraction process, varieties of raw plant materials, climate, geographical conditions and the sample preparation (Ohwoavworhua and Adelakun, 2005, Sohni et al., 2024) .

Organoleptically, both MK-MCC and MK-cellulose were white (Figure 4A and 4B), odorless, and tasteless. From texture perspective the MKcellulose had a fibrous structure while the MK-MCC was in the form of fine powders. The organoleptic properties of isolated MK-cellulose and MK-MCC met USP/NF requirements. The findings related to organoleptic properties and the yield of cellulose and MCC indicates that mango kernel fiber is a highly promising candidate for cellulose and MCC production.

A.  B. 

Figure 4: Cellulose isolated from mango kernel (A) & MCC isolated from mango kernel (B)

4.2. Characterization of Physicochemical Properties of MCC

4.2.1. Degree of Polymerization

In the cuprammonium hydroxide solvent, all cellulose MCC and Avicel PH 101 powder samples were completely soluble. The DP of cellulose samples is frequently determined using the intrinsic viscosities of cellulose solutions in cupper-ammonium hydroxide solution. The DP indicates the number of repeating glucose units in a polymer chain and used as an identification test for cellulose and MCC. MCC generally has DP values of less than 350, whereas native cellulose typically has values exceeding 10,000. Based on the cellulose sources and the isolation conditions (chemical concentration, temperature, and treatment period), these values vary considerably. As depicted in Table 1, MK-MCC had higher DP (312.4) and a molecular weight (50608.8 g/mol) than Avicel PH 101. The DP of MK-MCC was higher than the range reported by Melese *et al*. (2023) for MCC derived from Teff straw fiber (241.09–257.38). However, it was lower than the DP reported by Pachuau et al. (2019) for MCC from Ensete glaucum, which was reported as 323. This variation might result from differences in the extraction conditions, including the types and concentrations of chemicals used, the temperature, the treatment duration, and the nature of the raw materials (Hubbell and Ragauskas, 2010, Thielemans et al., 2022).

4.2.2. Water Soluble, Ether Soluble Substance, pH, Ash value, moisture content and hydration capacity

The values of water-soluble substance, ether-soluble substance, pH, ash content, moisture content, and hydration capacity of MK-MCC and Avicel PH-101 are shown in Table 1. The

percent of water-soluble substance, ether soluble substance, ash content and pH readings were within the acceptable range stated in USP/NF. There was no significant differences in all these value between MK-MCC and Avicel PH 101 (p> 0.05). The pH of both MK-MCC and Avicel PH 101 were nearly neutral which makes it suitable for the stability and physiological activity of pharmaceutical products. The pH of an excipient affects the solubility, stability, and physiological activity of most pharmaceutical formulations. The low ash values of MK-MCC (0.07%) and Avicel PH 101 (0.06%) indicate very low inorganic material content, and their ash content is consistent with pharmacopoeial specifications. The ash value represents the amount of residue remaining from a sample after it has been ignited, indicating the substance that does not volatilize during the combustion process (Vassilev et al., 2012).

Table 1: Water and ether soluble substance,moisture content, hydration capacity, ash value and pH of MK-MCC and Avicel PH 101

Test	MK-MCC	Avicel PH 101
DP	312.400 ±1.8	227.7
Molecular weight	50608.800 ± 2.1	36887.4
pH (5–7.5%)*	5.97 ± 0.057	6.02 ± 0.0208
Water soluble Substances (%) (≤ 0.25%)*	0.14 ± 0.043	0.11 ± 0.02646
Ether soluble substances (%) (≤ 0.05%)*	0.03 ± .006	0 .03 ± 0.003
Moisture content (%) [≤ 7%)*	3.47 ± 0.503	4.97 ± 0.15275
Hydration Capacity	2.7 ± 0.360	1.86667 ± 0.1764
Ash value (%) (≤ 0.1%)*	0.07 ± 0.010	0.06 ± 0.01

* = Pharmacopoeial accepted values.

The moisture content of MK-MCC and Avicel PH 101 (Table 1) powder is within the range of USP specification. The moisture content of MK-MCC was lower than Avicel PH 101 ($p<0.05$). The variability reflected in the moisture content values between MK-MCC and Avicel PH 101 preparations could be due to a higher initial moisture content of Avicel PH 101.

The MK-MCC exhibited significantly higher hydration capacity in contrast to the Avicel PH101. This discrepancy might be attributed to MK-MCC's lower initial moisture content and lower crystallinity. The percentage of moisture content increased as the relative humidity of the condition increased. Higher affinity for absorbing water from the environment is found in MCC powders with lower initial moisture content. This is because substances with lower moisture content have more available sites or surface areas capable of attracting and binding water molecules through physical adsorption. A lower crystallinity was shown to be correlated with increased water sorption because moisture sorption mostly happens in amorphous areas. The total amount of water adsorbed in a material has been reported to be proportional to the fraction of amorphous material contained. Compaction, tensile strength, powder flow, die-wall friction , viscoelastic characteristics of MCC and microbial growth in products during storage have all been found to be affected by moisture content. MCC's mechanical properties are altered and the tensile strength of MCC tablets decreases when its moisture content exceeds 5% due to the plasticizing effect of water molecules. When using MCC in a formulation containing pharmaceuticals that are susceptible to hydrolysis in the presence of moisture, the amount of moisture adsorbed may have an impact on the formulation's stability. Lower moisture levels are essential for safe storage, as higher moisture content can lead to microbial growth and subsequent degradation of quality (Tomar et al., 2017).

4.2.3. X-ray diffraction studies

Cellulose's amorphous and crystal parts may be distinguished by X-ray diffraction (XRD). To measure the crystallinity of the samples, XRD was performed and the crystallinity index (% CrI) value was calculated. Many OH groups found in cellulose interact with one another to produce intra- and intermolecular hydrogen bonds. The molecules are arranged in an orderly manner as a result of these hydrogen bonding, and cellulose exhibits crystalline formations. The diffraction pattern of crystalline cellulose exhibits strong signals with sharp peaks, whereas the amorphous (non-crystalline) component is characterized by weaker and wider signals. The degree of crystallinity affects a number of characteristics, such as water adsorption and compactibility. These could have an impact on the tablet product stability and flowability (Salem et al., 2023).

The Segal equation is commonly used to estimate the crystallinity index of cellulose materials based on their XRD patterns. The amorphous (I*am*) and maximum intensity (I*002*) peak

positions were located in the angle (*2-θ*) range of 18.18°–18.42° and 22.12°–22.5°, respectively. Differences in peak height and width are observed between the samples due to differences in their degree of crystallinity and crystal size. The CrI of MK-Celulose and MK-MCC and Avicle PH 101 (Table 2) were found to be 76.45%, 82.27%, and 86.85% respectively. In this study, the crystallinity of MK-MCC was found to be higher compared to MCC derived from giant reed (79.1%) as isolated by Tarchoun AF *et al*,(2020) and MCC from date seeds of palm trees (70%) as isolated by Abu-Thabit NY *et al* (2020). The CrI of MK-MCC falls within the typical range of crystallinity observed in commercial MCC, which ranges from 55% to 80%. CrI of MCC depends on nature of the plant fibers and the conditions used for isolation (Sainorudin et al., 2018).

These increase of crystallinity index and sharpening of XRD peaks (Figure 14) might be due to elimination of amorphous lignin and hemicellulose through delignification, alkali treatment, bleaching, and hydrolytic cleavage of glycosidic bonds by HCl acid. The degree of crystallinity increased aproximatley by 8% due to removal of the amorphous regions of cellulose by acid hydrolytic cleavage. The crystallinity increased with decreased DP because the crystallites surface corresponding to amorphous cellulose regions diminished (Kim et al., 2010).

Table 2: Crystallinity index of MK-Cellulose, MK-MCC and Avicel PH 101

Parameters		**MK-cellulose**	**MK-MCC**	**Avicel PH 101**
Peak position 2θ(°)	I002	22.12	22.5	22.5
	Iam	18.18	18.38	18.42
Intensity (a.u)	I002	1818	2414	2526
	Iam	428	428	332
CrI(%)		76.45± 0.34	82.27±0.2	86.85±14

CrI: Crystallinity index

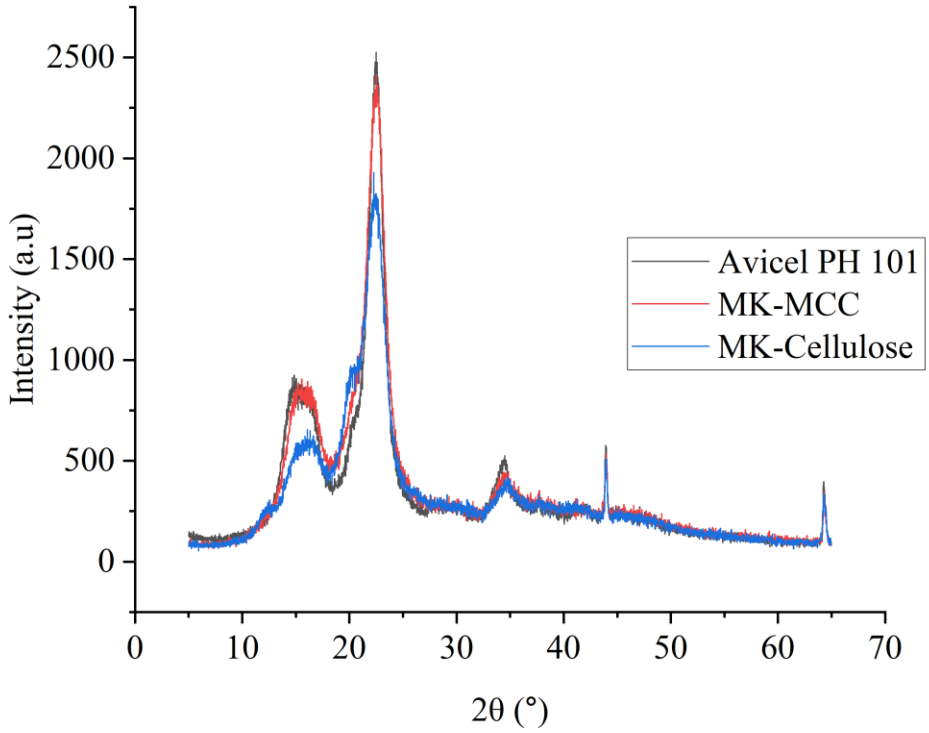

Figure 5: XRD patterns of MK-cellulose, MK-MCC and Avicel PH 101 powder

4.2.4. Scanning electron microscopy

The morphological and textural characteristics of MK-raw fiber MK-Cellulose, MK-MCC and Avicel PH 101 (Figure 6) were examined by SEM analysis. SEM micrographs showed changes in the morphology of samples in terms of shape, size and level of smoothness after acid hydrolysis. Because hemicellulose, lignin, and other non-cellulosic materials cover the surface of cellulose, the SEM picture of the raw MK fiber shows a rough surface. The MK-cellulose and MK-MCC shows irregular smooth rod shape fiber strands.

The MK-MCC exhibited a smoother surface and shorter length compared to the raw fiber and its cellulose. This is attributed to the removal of hemicellulose, lignin, and other impurities, as well as the breakdown of fibrous strands into smaller microcrystallites during the HCl treatment. Removal of lignin and the amorphous area of cellulose results in the formation of irregularly rod shaped MCC particles which is similar to the findings of various study. This finding aligns with

results reported by Lalduhsanga Pachuau *et al* (2014) and Nkemakolam Nwachukwu *et al* (2018) (Nwachukwu and Ofoefule, Pachuau et al., 2014).

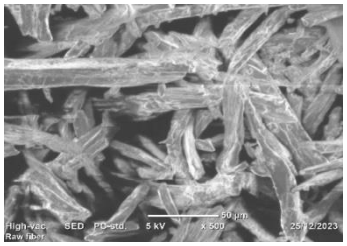

(A)

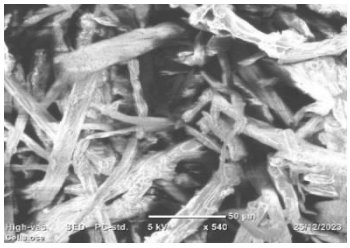

(B)

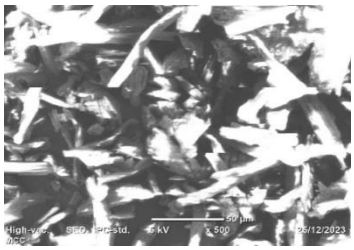

(C)

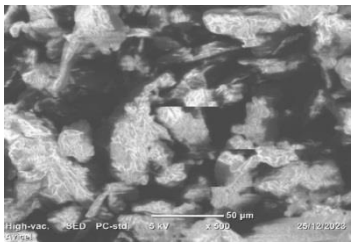

(D)

Figure 6: SEM micrographs of MK-fiber (A), MK-cellulose (B) MK-MCC (C) and Avicel PH 101 (D) at 500x

4.2.5. Thermal stability study

TGA and DTG are commonly used methods to investigate the thermal and degradation properties of polymers by determining mass change in the polymer as a function of time and temperature. For characterizing heterogeneous organic materials, it is a convenient, reproducible, and beneficial approach. The primary determinants of the breakdown temperature of cellulose and MCC are their molecular weight and purity (Chaerunisaa et al., 2019). Furthermore, the degree of crystallinity and polymer morphology have an impact on the decomposition temperature; a polymer with a high degree of crystallinity would have a higher decomposition temperature (Kim et al., 2010).

TGA (Figure 7) and DTG (Figure 8) curves of the samples show three weight loss regions. The first stage weight loss was observed in the temperature range of 51-159 °C, 52-137 °C and 52-

158 °C MK-Cellulose, MK-MCC and Avicel PH101 with corresponding weight loss of 9.21 ± 0.75%, 4.18 ± 0.21%, and 9.17% ± 0.10 respectively. The weight loss in this region of 51- 159 °C is mainly due to moisture evaporation. The rate of temperature for water evaporation depends on the original moisture content of the sample (Heng et al., 2004). The weight loss of MK-cellulose and Avicel PH 101 were higher compared to MK-MCC powder in this region ($p<0.05$). This could be due to due to high initial moisture content. The temperature at which 10% of the material is degraded (T10%) is in increasing order of MK-cellulose (170.85 °C), Avicel PH-101 (170.35°C) and MK-MCC (338.85 °C) ($p <0.05$). The amount of loss might be correlated with their respective amount of moisture content (Trache et al., 2014).

The second and major decomposition peak was observed at about 227-445 °C, 292-390 °C, 294-394 °C for MK-Cellulose, MK-MCC and Avicel PH101 respectively. Higher proportions of all the samples were degraded in this decomposition stage. Decomposition in this region was due to depolymerization, dehydration and decomposition of the glycosidic units of cellulose. The major constituents of natural fiber: cellulose, hemicellulose, lignin, and ashdecompose at these temperatures ranges. Hemicelluloses break down early at temperatures below 400 ◦C, and lignin then undergoes pyrolysis. In this stage 53.69 ± 1.2%, 67.65 ± 0.4% and 61.78 ± 0.32% of MK-cellulose, MK-MCC and Avicel PH 101 were degraded respectively. MK-cellulose show lowest degradation in this stage ($p<0.05$). Since hemicelluloses and cellulose components degradation is responsible for weight loss in this region whereas its higher lignin content degraded later which is mainly responsible for the char formation (Werner et al., 2014).

The char residues of MK-cellulose, and MK-MCC and Avicel PH 101 at 700 °C were 13.56%, 7.46%, and 4.6% respectively. The process of converting biomass into a solid residue with an aromatic polycyclic structure results in formation of char. Among lignocellulosic compounds, lignin and hemicellulose cause a significant amount of char formation. MK-cellulose show the highest char residue (13.56 ±1.3%) which could be attributed to the presence of more amounts of lignin and ash (Collard and Blin, 2014).

As depicted in DTG curve (Figure 8) MK-MCC and Avicel PH101 each displayed a small endothermic peak at 104 °C and 102 °C, respectively, corresponding to water evaporation, as confirmed by TGA results. Additionally, both MK-MCC and Avicel PH101 showed a second large endothermic peak at 367 °C and 345 °C, respectively, which is attributed to the second

stage of decomposition. This endothermic peak in this temperature range aligns with the rapid weight loss observed in the TGA curve (Werner et al., 2014).

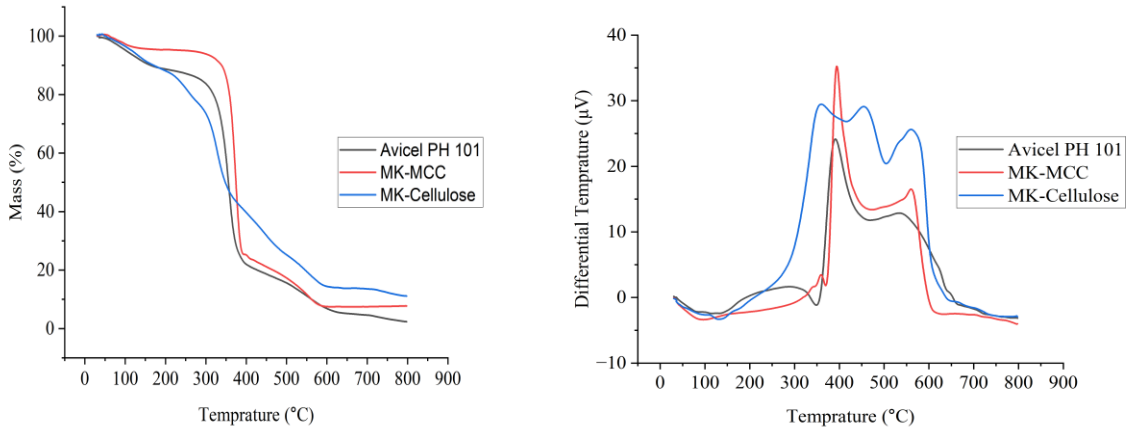

Figure 7: TG curve (A) and DTG curve (B) of MK-cellulose, MK-MCC and Avicel PH 101

4.2.6. Moisture sorption

Moisture is known to affect the mechanical properties and functionalities of powders such as flow, compressibility and tablet strength. The amorphous portion of MCC is considered to be responsible for moisture absorption, hence increased degree of crystallinity will result in lower moisture absorption. The extent of water adsorption by cellulosic material is proportional to the amount of amorphous cellulose present. The study of the moisture content capacity of MCC is important because it affects the stability of pharmaceutical products during storage and transportation under humid conditions. The moisture sorption investigation showed that water absorption increased with increased relative humidity (RH) (Veronica et al., 2022).

MK-MCC showed (Figure 8) significantly higher moisture absorption than Avicel PH 101($p<0.05$) at all levels of relative humidity due to its lower degree of crystallinity and lower initial moisture content. Higher moisture sorption indicates a greater potential for moisture absorption during storage, which can adversely affect product quality. Moisture contents of MK-MCC and Avicel PH 101 exceeded the acceptable limit set for MCC (6%) above 40% RH. Therefore, the humidity of storage and operation conditions of MK-MCC powders need to be monitored strictly (Mihranyan et al., 2004).

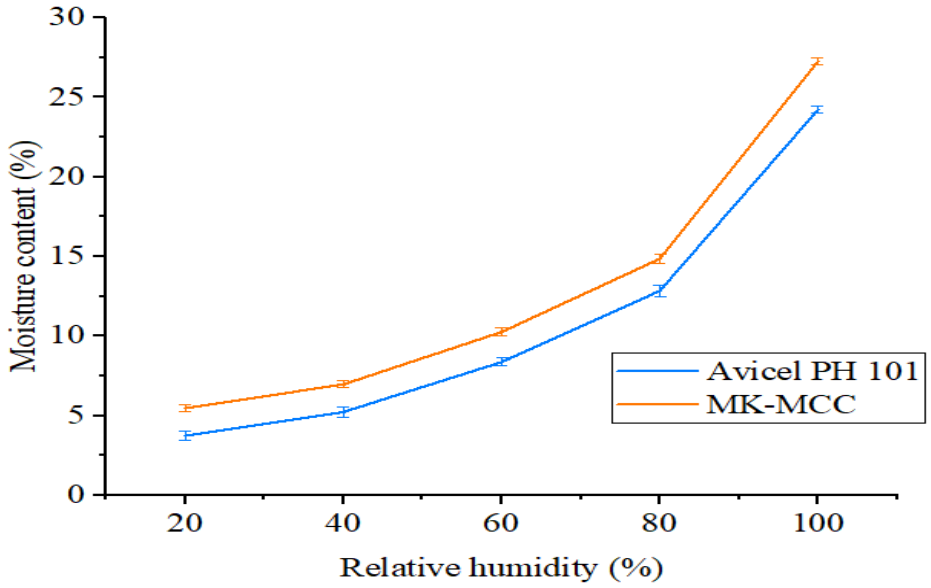

Figure 8: Moisture sorption pattern of MK-MCC and AvicelPH 101

4.2.7. Density and related properties of MCC

4.2.7.1. Bulk, Tapped and True Density

As shown in Table 2, MK-MCC showed a lower bulk and tapped density ($p<0.05$) than Avicel PH101 . The bulk density of MK-MCC is comparable with the reported bulk density of bagasse MCC (0.32 g/ml) and is less than that of cotton stalk MCC (0.59 g/ml). Lower bulk and tap density of MCC could be due to its lower crystallinity. Flow and the compaction profile of a material can be understood through bulk and tapped densities. The bulk density gives an estimation about flow properties of material while the tap density measures compaction properties of materials. Materials with higher bulk and tapped density have better flow properties. Lower bulk densities of powders indicate higher porosity and make them easier to compress, but they may also interfere with the powder's ability to flow freely. Particle size, particle size distribution, particle shape and the tendency of the particles to adhere to one another affects powder's bulk density. Variations in bulk and tapped densities may also be caused by variations in the crystallinity index and moisture content (Zuliahani et al., 2016).

The true density of MK-MCC (Table 3) was slightly lower compared to Avicel PH101 ($p>0.05$). The true density of a material is defined as the average mass of the particles divided by the solid

volume, excluding any voids that are not an integral part of the molecular packing structure. The true density of 100% crystalline natural cellulose ranges from 1.582 to 1.599 g/cm³. Since the crystallinity of MCC had far less than 100%, the true density of MCC is expected to be lower than 1.582 g/cm^3. As the degree of crystallinity of MCC increases the true density of MCC also increases (Pachuau et al., 2013).

Table 3: Density related properties of MK-MCC and Avicel PH 101

Powder properties	MK-MCC	Avicel PH 101
Bulk density (g/cm3)	0.30 ± 0057	0.35 ± 0.0057
Tapped density (g/cm3)	0.39 ± 0 .010	0.45 ± 0 .0057
True density (g/cm3)	1.54 ± 0.02	1.57 ± 0.01
Carr's index (%)	22.88 ± 0.33	20.15 ± 1.1622
Hausner ratio	1.29 ± 0.0208	1.25 ± 0.0157
Porosity (%)	80.21 ± 0.453	77.27± 0.3897

4.2.7.2. Carr's index and Hauser ratio

Carr's index (CI) and Hausner's ratio (HR) are regarded as indirect indicators of powder compressibility and flowability and calculated from bulk and tapped densities. Hausner ratio values ranging from 1.001 to 1.11, 1.12 to 1.18, 1.19 to 1.25, 1.26 to 1.34, and 1.35 to 1.45 correspond to flow properties classified as excellent, good, fair, passable, and poor, respectively. Conversely, Carr's index classifies powder flow characteristics as excellent (≤10%), good (11–15%), fair (16–20%), passable (21–25%), poor (26–31%), and very poor (32–37%) (USP, 2007). The HR and CR result indicates that MK-MCC had passable flow and compressibility properties. Flow properties of MCC could be affected by moisture content, particle size, particle shape, particle size distribution and intra/inter-particulate forces among particles (Tan et al., 2015). The HR and CI of MK-MCC was found to be 1.29 and 22.88 respectively (Table 3). The Carr index and Hausner ratio values of MK-MCC were higher compared to Avicel PH 101. This could be attributed to a, increased porosity of MK-MCC (Shah et al., 2008).

4.2.7.3. Porosity

Porosity is inter- and intra-void spaces of particles. Particle morphology, packing structure, and size range variations are the common factors that influence powder porosity. The bulk, tapped, and true densities of the powder can also affect porosity. Powder porosity is inversely related with bulk and tap densities of powder. MK-MCC was found to be more porous compared to Avicel PH 101 ($p<0.05$). This could be due to its lower bulk, tapped density and lower crystallinity of MK-MCC (Kothari et al., 2002).

4.2.8. Particle size analysis

As shown in Table 4, the D10 and D50 of MK-MCC were much lower than those of Avicel PH 101, whereas the D90 was significantly higher, where D10, D50, and D90 stand for 10, 50, and 90 cumulative percent undersize, respectively. The D10, D50, and D90 of Avicel PH-101 are specified by the FMC Specification to be within the ranges of 14–30, 40–75, and 77–156 μm, respectively. In this result only D90 of both sample was within acceptable range. In comparison to Avicel PH 101, MK-MCC was also shown to have a much larger relative span. Relative span, which is the ratio of the difference between D90 and D10 and M50, determines the breadth of the distribution. Span value <1, 1-3, and > 3 represents narrow, moderate and wide particle size distribution respectively. According to this result, MK-MCC has moderate particle size distribution. A wider particle size distribution, with a range of particle sizes, can lead to poor flow properties compared to a narrower distribution. Avicel PH 101 (Figure 10) had monomodal particle size distribution whereas MK-MCC (Figure 11) had a bimodal particle size distribution. The grinding process of MK-MCC powder may not uniformly reduce all particles to a single size. Instead, it can result in the creation of smaller particles while some larger particles remain, leading to a bimodal distribution. Aggregation of MCC particle as a result of moisture content, electrostatic forces, or inadequate drying procedures could also form larger particles, and resulting in a secondary mode in the particle size distribution (Li et al., 2022)

MK-MCC had larger mean particle size than Avicel PH 101. This discrepancy may be due to the difference in milling processes, screening and sieving processes, method and conditions used for drying and storage conditions. According to FMC (2003), the MCC's mean particle size must be in the range of 35-50 μm. The mean particle size of MK-MCC in this investigation satisfied the

FMC requirement. The specific surface area of MK-MCC was higher than that of Avicel PH 101. Greater specific surface area of MK-MCC may be due its higher porosity and lower crystallilnity index. This correlation arises because of a material with higher porosity and lower crystallinity has more internal surfaces and voids, which increases the surface area per unit mass of the material . Overall, this study found that MK-MCC exhibited a moderate particle size distribution and an appropriate mean particle size, making it a good candidate for use as a direct compression excipient (Gamble et al., 2011).

Table 4: Particle size and size distribution of MK-MCC and Avicel PH 101

Parameters	MK-MCC	Avicel PH 101
Mean particle size (µm)	45.17± 0 .6928	42.26 ± 0 .3345
D_{10} (µm)	6.68 ± 0.1135	7.54 ± 0.1777
D_{50} (µm)	31.13 ± 0.3401	32.75 ± 0.2971
D_{90} (µm)	100.61 ± 1.72047	75.72 ± 0.6143
SSA (m^2/g)	0.55 ± 0.0046	0.28 ± 0.0036
Span	3.00 ± 0.0461	2.085 ± 0.0140

M10, M50, and M90 represent 10, 50 and 90 cumulative percent undersize, respectively,

SSA: Specific surface area, Span= (D90 - D10)/D50

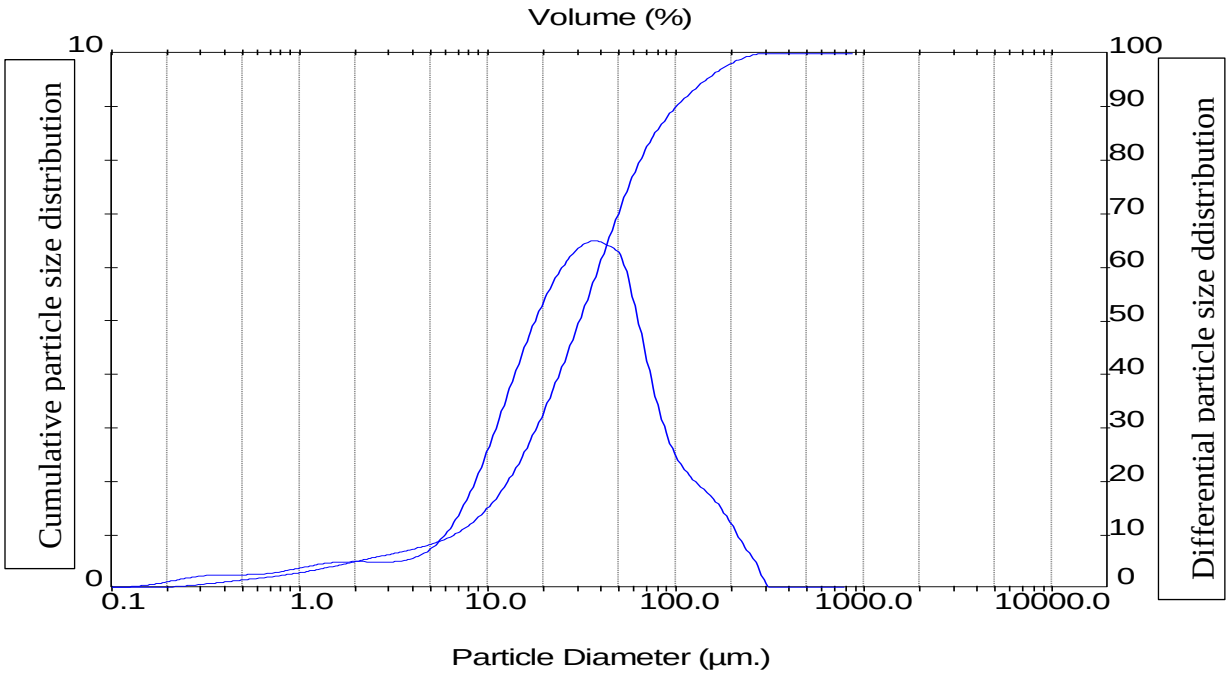

Figure 9: Volumetric particle size distributions of Avicel PH 101

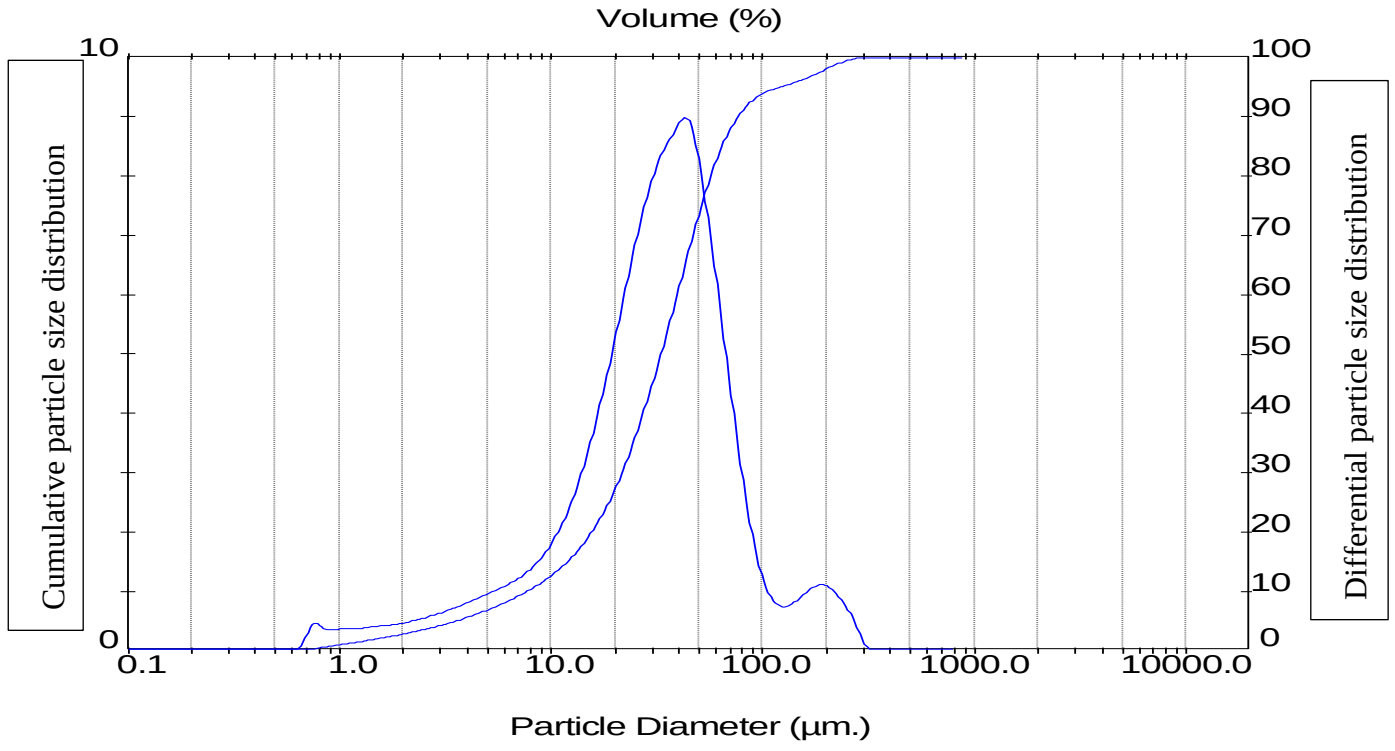

Figure 10: Volumetric particle size distributions of MK-MCC

4.2.9. FTIR and Drug-excipient compatibility study

4.2.9.1. FTIR Study

In FTIR spectra (Figure 12-14), the two primary absorbance zones are found at low wavenumbers (–1700-500cm^{-1}) and high wavenumbers (3500–2800 cm^{-1}). The stretching vibration of OH groups was responsible for the wide absorption band seen in all samples at 3300 cm^{-1}. Stretching vibrations of the CH are indicated by the other peaks at round 2890 cm^{-1}. The bending mode of the absorbed water is most likely responsible for the absorption band around 1650 cm^{-1} in all samples. An aromatic ring stretch that is closely linked to the aromatic C-O stretching band is responsible for the peak at 1595 cm -1. The disappearance of the absorption peaks around 1730 cm−1 and 1533 cm−1 for CO stretching of the acetyl and uronic ester groups of hemicellulose or the ester linkage of carboxylic groups of ferulic and p-coumaric acids of lignin, respectively, confirmed the removal of hemicellulose and lignin in all celluloses and MCC (Kunusa et al., 2018, Trache et al., 2013).

The bands located at 1314, 1317, and 1318 cm-1 correspond to either the –CH or –CH_2 vibrations linked to intermolecular hydrogen bonds at the C group or the OH in plane bending vibration. The C-O-C asymmetrical stretching of β-1,4-glycosidic linkage is responsible for the peak values seen at 1159 cm-1 MK-MCC molecules. The C-O-C pyranose ring skeletal stretching is shown by the other notable peak at 1028, 1029, and 1033 cm^{-1}. The glycosidic C1–H deformation with ring vibration contribution and O–H bending, which is typical of β-glycosidic connections between glucose in cellulose, might be responsible to a short sharp peak at around 890 cm-1. The cellulose and MCC displayed similar spectra indicating that the chemical compositions of all the samples are the same (Kunusa et al., 2018).

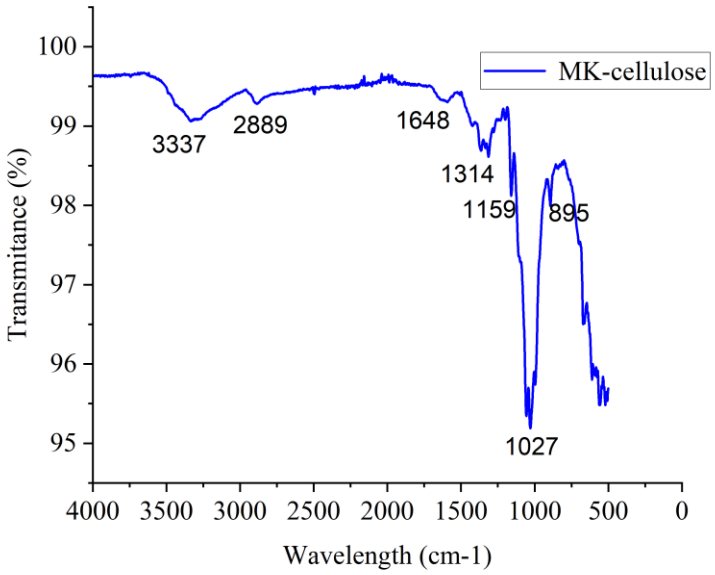

Figure 11: FTIR spectra of MK-cellulose

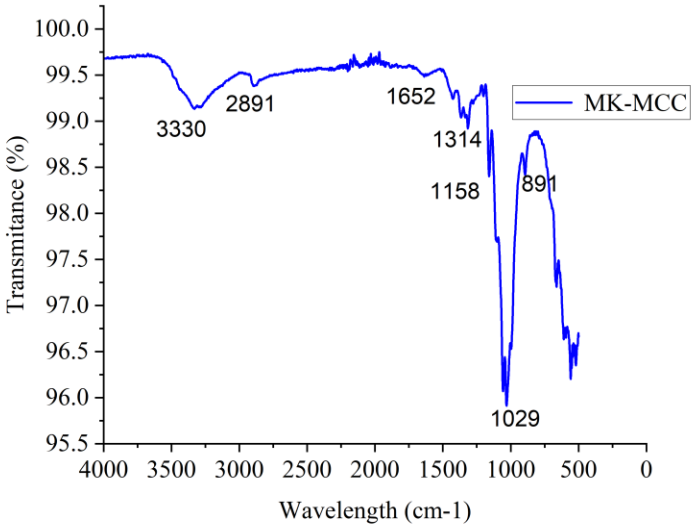

Figure 12: FTIR spectra of MK-MCC

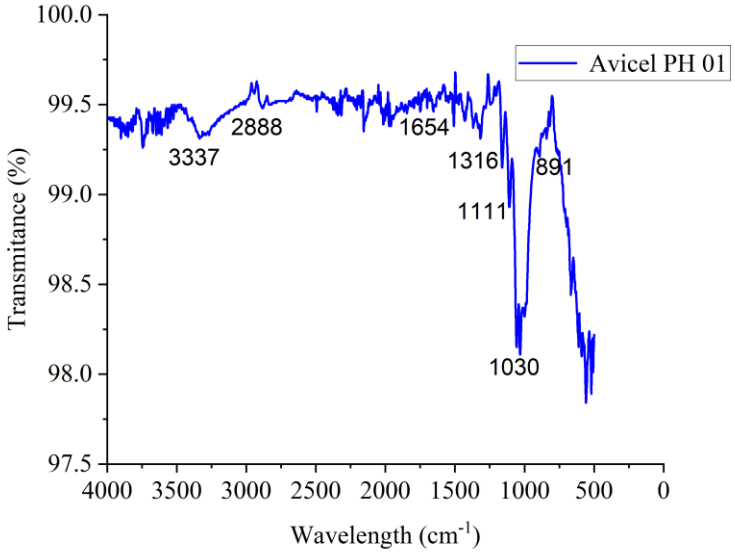

Figure 13: FTIR spectra of Avicel PH 101

4.2.7.2. Drug-excipient compatibility study

Drug-Excipient compatibility studies were conducted to evaluate interaction between paracetamol and MK-MCC physical mixture. As depicted in Figure 14 and 15 the peak around 3324 cm-1 and 1652 cm^{-1} shows presence of O-H stretching and C-O stretching vibration respectively. The symmetrical bending in C-H and C-N (aryl) stretching was attributed to the absorption peaks at 1367 and 1323 cm-1. Additionally the absorption peaks at 1170 and 968 cm-1, respectively, were attributed to C-O and C-N (amide) stretching. When compared to the spectrum data of the paracetamol & MK-MCC mixture, the absorption bands for paracetamol and MK-MCC stayed unaltered. These indicates that there is no compatibility issues between MK-MCC and paracetamol (Mallah et al., 2015).

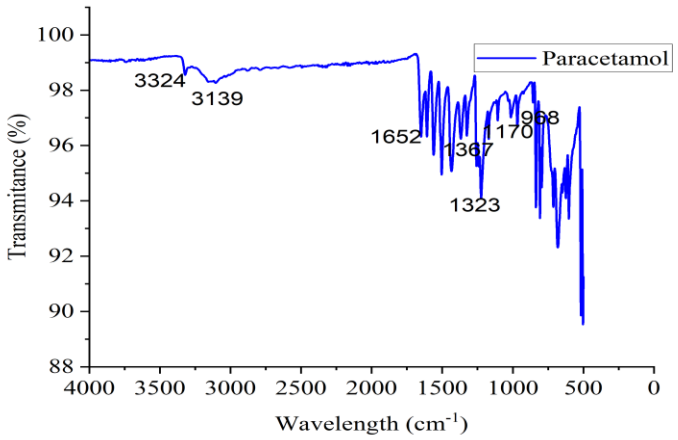

Figure 14: FTIR spectrum of paracetamol

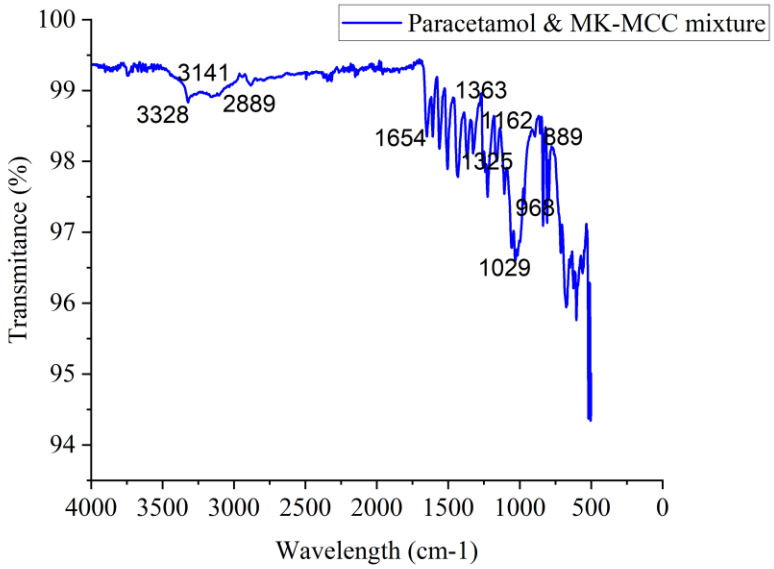

Figure 15: FTIR spectrum of mixture of paracetamol & MK-MCC(1:1) mixture

4.3. Direct Compression and Evaluation of Tablet properties

4.3.1 Compactability properties

4.3.1.1. Weight, thickness and diameter of plain MCC tablet

Microcrystalline cellulose is one of the most widely used filler-binders in direct compression. As a dry binder excipient, it offers the highest capacity and compressibility among all direct compression agents. An excellent balance between high plasticity, low brittleness, viscoelasticity, and particle interlocking produces its exceptional compressibility. Its excellent bonding properties as a dry binder account for its widespread use in direct compression (Zhao et al., 2022).

The weight of tablet made from Avicel PH 101 were significantly higher compared to MK-MCC tablet ($p < 0.05$). This could be result from higher crystallinity and bulk density of Avicel PH 101. The weight variation of both MK-MCC and Avicel PH 101 tablet were in the accepted range. Thickness of tablet decreased with increment of compression forces in both MK-MCC and Avicel PH 101 tablets (Table 5). This may be due to tighter packing and reduced porosity of powder caused by increased compression forces (Zuliahani et al., 2016).. Thickness of tablets prepared from both MK-MCC and Avicel PH 101 powder was comparable ($p>0.05$).

Table 5: Weight, Thickness and Diameter of plain tablets of MK- MCCs and Avicel PH101.

Sample	**Parameters**	**Compression force**				
		CF1(50N)	CF2(75N)	CF3(100N)	CF4(125N)	CF5(150N)
MK-MCC	Weight(MG)	389.17± 0.95	389.60 ± 0.20	388.80 ± 0.435	389.03 ± 0.305	389.40 ± 0.781
	Thickness (mm)	6.043 ± 0.06	5.69 ± 0.02	5.35 ± 0.010	5.14 ± 0.0305	4.99 ± 0.010
	Diameter (mm)	10.90 ± 0.02	10.89 ± 0.005	10.90 ± 0.010	10.90 ± 0.011	10.90 ± 0.010
Avicel PH-101	Weight (mg)	393.36 ± 0.3	393.56 ± 0.89	393.96 ± 0.838	393.90 ± 0.60	393.30 ± 0.346
	Thickness (mm)	6.06 ± 0.055	5.70 ± 0.0152	5.34 ± 0.0208	5.11 ± 0.010	5.01 ± 0.012
	Diameter (mm)	10.90 ± 0.02	10.91 ± 0.01	10.90 ± 0.015	10.90 ± 0.0057	10.89 ± 0.005

4.3.1.2. Crushing strength, Tensile strength of plain MK-MCC tablets

Crushing strength measurements gives an indication of the ability of tablets to withstand pressure and can be a useful tool for the selection potential of direct compression excipients whereas tensile strength gives indication about the strength of a tablet and it may provide information about the laminating and capping tendencies of the material. The crushing strength of tablets made from Avicel PH 101 was found to be higher compared to tablets of MK-MCC ($p<0.05$). This is due to Avicel PH 101's greater bulk density, lower DP, and higher crystallinity index when compared to MK-MCC. According to literature evidence, crushing strength generally increases with decreased DP of powder, with increasing crystallinity index and with decreasing particle size (Li et al., 2022).

According to the USP specification, directly compressible tablets should have a hardness ranging from 4 to 10 kN (40-100 N). In this study MK-MCC tablets generally exhibited hardness values within this permissible range, except for those compressed at CF-50 and CF-150 N, which did not meet the specification. Similarly, Avicel PH 101 tablets showed hardness values within the acceptable range, except for those compressed at CF-125 and CF-150 N. Tensile strength increased with crushing strength of tablet. The tensile strength of Avicel PH-101 was greater than MK-MCC tablets at all level of CFs ($p<0.05$) (Figure 17). This higher tensile strength might be correlated with higher crystallinity and higher bulk density (Kothari et al., 2002).

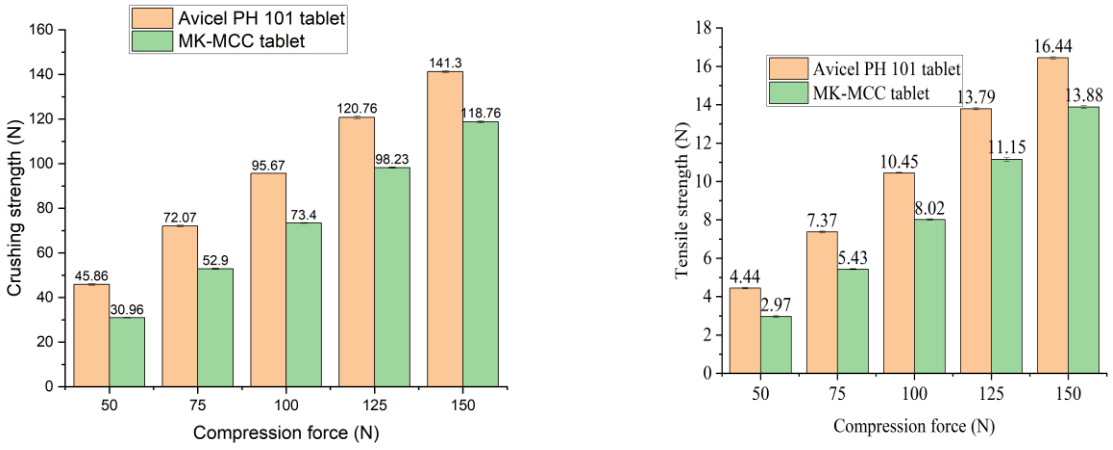

Figure 16: Crushing strength (A) and Tensile strength (B) of plain tablets of MK- MCC and Avicel PH101

4.3.1.3. Friability of Plain MK-MCC Tablets

Friability test is done in order to monitor the resistance of tablets to stresses like mechanical shocks and abrasion during the manufacturing, packing and transportation processes. In the friability test, tablets that lose not more than 1% of their weight are often considered as acceptable (Osei-Yeboah and Sun, 2015). In this study, friability of tablet of MK-MCC and Avicel PH101 decreased with an increase in compression force ($p<0.05$) (Figure 18). This might be due to increment of inter-particulate cohesiveness with increasing in compression force. Avicel PH-101 had significantly low value of friability than MK-MCC at all compression forces ($p<0.05$). This could be due to its higher crushing and tensile strength of tablet. At all compression force levels, tablets made with Avicel PH101 and MK-MCC showed acceptable weight losses during the friability test except MK-MCC tablet at compression force of 50N (Begat et al., 2005).

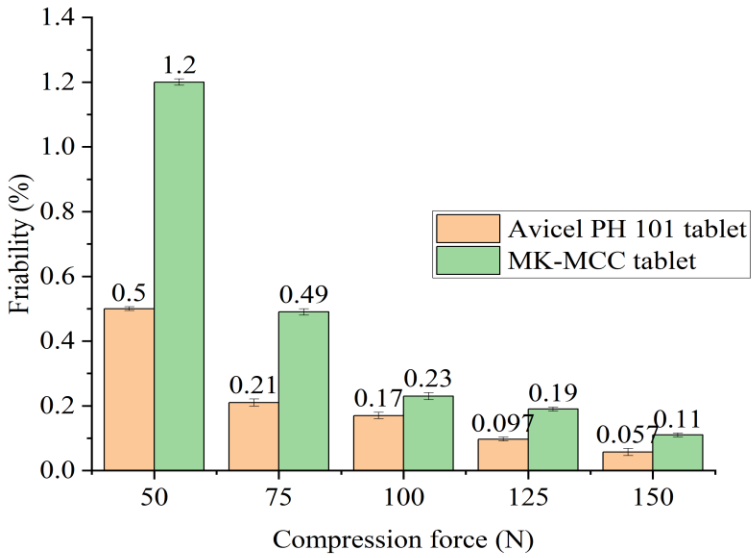

Figure 17: Friability of plain tablets of MK- MCC and Avicel PH 101

4.3.1.4. Disintegration time

According to British Pharmacopeia the disintegration time limit of conventional drugs is less than 15 minutes. The disintegration time increased with an increase in compression force for tablet preparations from both type of powders (Figure 19). Avicel PH-101 tablets showed prolonged disintegration time than MK-MCC ($p<0.05$). This could be as a result of the harder tablets made from Avicel PH101 at all compression force levels compared to MK-MCC. Additionally, lower swelling capacity due to lower hydration capacity may have contributed to longer Avicel PH 101 disintegration time. The smaller specific area of Avicel PH101 might prolonged disintegration time as compared to MK-MCC. A lower degree of crystallinity of MK-MCC might also made it easier for water molecules to enter and interact with free hydroxyl groups (Kumar et al., 2001). Tablets prepared from both powders had disintegration time in acceptable range (<15 min) at all compession forces (50-150N).

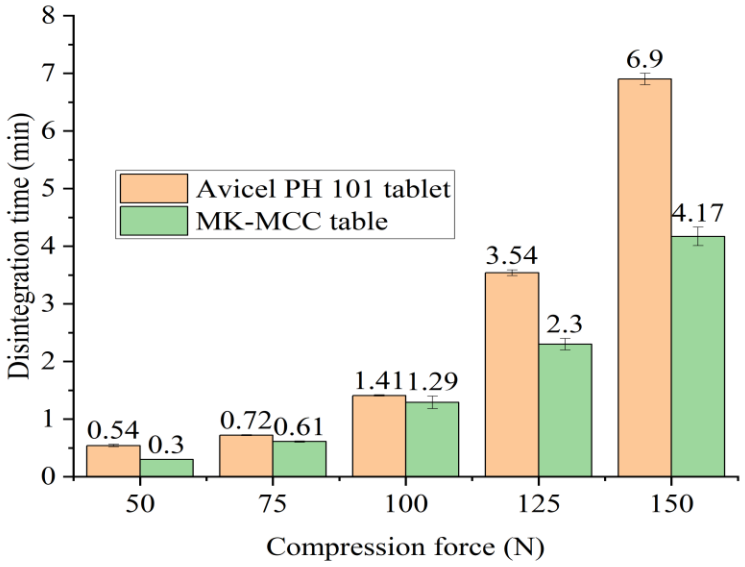

Figure 18: Disintegration time of plain tablets of MK- MCC and Avicel PH101

4.3.2. Lubricant Sensitivity

Products are considered as very sensitive to the lubricant used if their Lubricant Sensitivity Ratio (LSR) values are near to unity. Crushing/tensile strength tablet of MCC powders is decreased upon addition of magnesium stearate (0.5%) due to formation of weaker bonds, after compression, between lubricant-lubricant molecules rather than strong excipient-excipient bonds. One of the lubricants most frequently used in the manufacturing of tablets is magnesium stearate. It is relatively inexpensive, has low friction coefficient, high covering, and provides high lubrication potential (Rajani et al., 2018).

In this study hardness of MK-MCC and Avicel PH 101 tablet was reduced upon addition of magnesium stearate (0.5%) compared to unlubricated plain MK-MCC tablets ($p<0.05$) (Table 6). This might be due to the fact that the magnesium stearate particles may disrupt the interaction bonding forces that hold the MCC particles together, thus weakening the tablets' overall strength. Avicel PH 101 was more lubricant sensitive than MK-MCC ($p<0.05$). The reason could be due to its less porous structure and the high bulk density of Avicel PH101 compared to MK-MCC which facilitates the formation of a continuous lubricant film. The higher LSR is the consequence of limited porosity and high bulk density, which provide less void space for lubricants. Powder with better flowability is known to be more lubricant sensitive (ALFA, 2008).

Table 6: Impact of magnesium stearate (0.5%) on hardness of tablets and LSRs

Sample	**Crushing strength**		**LSR**
	Unlubricated plain tablet	Lubricated tablet	
MK- MCC	73.03 ± 0.20817	63.6± 0.34641	0.129 ± 0.0026
Avicel PH-101	97.03 ± 0.46188	78.2 ± 0.52915	0.194 ± 0.002

4.3.3. Tablet compressed from MCC powder loaded with paracetamol

4.3.3.1. Weight, Thickness and Diameter of directly compressed Paracetamol Tablet

Dilution potential of MK-MCC and Avicel PH-101 was assessed by using paracetamol as a model drug at a fixed compression force (100N). The weight, thickness and diameter of tablets prepared from MK-MCC and Avicel PH101 powders are presented in Table 7. The thickness of tablet of both MK-MCC and Avicel PH 101 formulations did not show any significant variations ($p > 0.05$). The weight of tablet made from Avicel PH 101 were significantly higher compared to MK-MCC tablet ($p < 0.05$) at all paracetamol concentration (35,50,65,80%). This could be result from higher crystallinity and bulk density of Avicel PH 101 powder. Weight of tablets increased with increasing concentration of paracetamol in both MK-MCC and Avicel PH-101 tablets ($p<0.05$). This could be due to higher bulk density of paracetamol, therefore, as the concentration of paracetamol increased the weight of tablet increased (Zuliahani et al., 2016).

Table 7: Weigth, thickness and diameter of directly compressed MK-MCC and Avicel PH101 tablets loaded with different percentage of paracetamol

Sample	**Tablet parameter**	**Paracetamol concentration (%)**			
		35	50	65	80
MK-MCC	Weight(mg)	390.06± 0.23	391.56 ± 0.152	392.66 ± 0.1527	393.34 ± 0.153
	Thickness (mm)	4.98 ± 0.010	4.98 ± 0.0153	4.97 ± 0.012	4.99 ± 0.0116
	Diameter (mm)	10.91 ± 0.012	10.90 ± 0.01	10.91 ± 0.012	10.90 ± 0.01
Avicel PH-101	Weight (mg)	393.33 ± 0.152	393.90 ± 0.264	394.83 ± 0.493	394.80 ± 0.0577
	Thickness(mm)	4.98 ± 0.006	4.98 ± 0.0057	4.98 ± 0.010	4.98 ± 0.006
	Diameter(mm)	10.90 ± 0.0153	10.92 ± 0.0058	10.91 ± 0.01528	10.90 ± 0.02

4.3.3.2. Crushing strength of directly compressed Paracetamol Tablets

The crushingg strength and tensile strength of paracetamol tablets showed a significant decrement ($p<0.05$) as the concentration of paracetamol increased in tablets produced with MK-MCC and Avicel PH101 as diluents. This might be caused by poor compressibility and elastic recovery of paracetamol. Tablet formulations at all concentration of paracetamol prepared with Avicel PH-101 showed significantly higher crushing strengths and tensile strength than those prepared with MK-MCC ($p < 0.05$). This may be due to Avicel PH 101's higher bulk density, lower DP, and higher crystallinity index compared to MK-MCC. Crushing strength generally increases with a lower DP , a higher crystallinity index and smaller particle size (Shlieout et al., 2002).

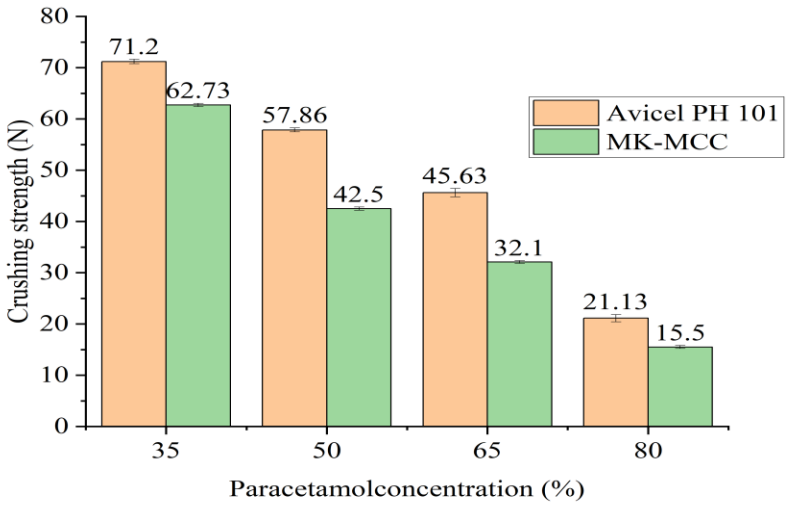

Figure 19: Crushing strength of directly compressed MCC tablets loaded with different percentages of paracetamol

4.3.3.3. Friability of Directly compressed Paracetamol Tablets

Friability of MK-MCC and Avicel PH 101 tablets increased significantly with increased concentration of paracetamol ($p<0.05$). The reason for increment of friability may be the reduction of hardness of tablets as the result of higher concentration of poor compressiblility of paracetamol. The friability of paracetamol tablets containing MK-MCC and Avicel PH-101 were in the acceptable range (< 1%) except for MK-MCC tablets with 65% and 80% drug content.

The low crushing strength values coupled with poor compressibility of paracetamol might contributed to high friability of tablets containing 65% and 80% of paracetamol formulations. Avicel PH-101 had significantly low value of friability than MK-MCC at all levels of paracetamol concentration ($p<0.05$). This could be due to its higher crushing and tensile strength of Avicel PH 101 tablets (Paul and Sun, 2017).

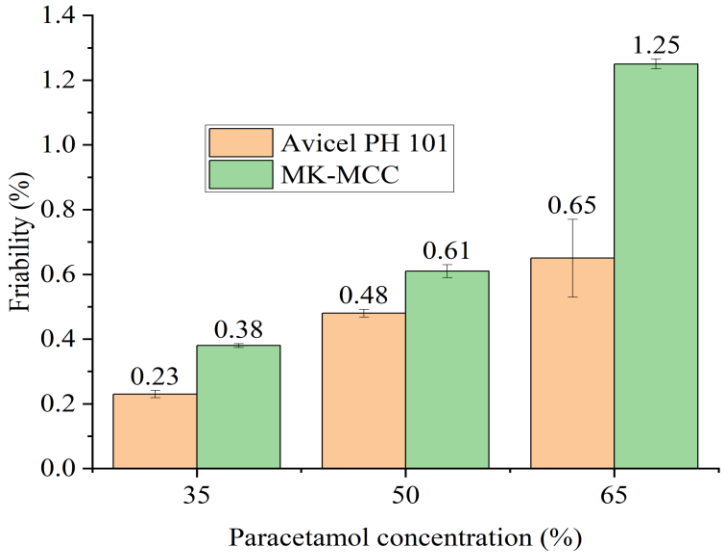

Figure 20: Friability of directly compressed MCC tablets loaded with different percentages of paracetamol

4.3.3.4. Disintegration of directly compressed paracetamol Tablets

The disintegration test indicates the time required for a tablet to break into many small particles with a much greater total surface area than the intact tablet. In this study, the disintegration time of the tablets decreased as the paracetamol concentration increased. Reduction of disintegration times might be explained by decreasing of tablet hardness as result of paracetamol content increment. In this study, the disintegration times of paracetamol prepared from MK-MCC and Avicel PH-101 tablets were less than 15 min, which is recommended for conventional dosage forms in the USP/NF specification. However, Avicel PH-101 shows the delayed disintegration time than MK-MCC ($p<0.05$). This may be due to higher crystalinity index and low porosity values of Avicel PH 101 (Yassin et al., 2015).

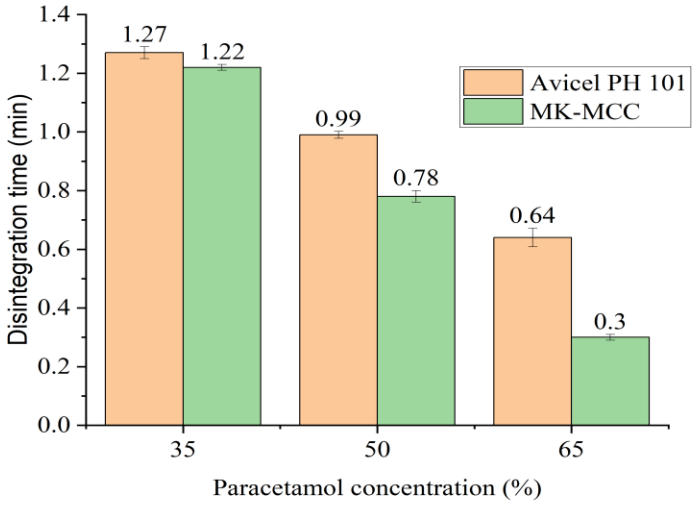

Figure 21: Disintegration of directly compressed MCC tablets loaded with different percentages of paracetamol

4.3.3.5. Dilution capacity

Dilution potential refers to the capacity of directly compressible excipients to accommodate high concentrations of an active pharmaceutical ingredient. It measures the proportion of a poorly compactible drug that can be incorporated into an excipient while still producing tablets with satisfactory mechanical strength. Dilution potential is influenced by the compaction behavior of both the excipients and the active pharmaceutical ingredient. The dilution potential of MK-MCC was assessed using paracetamol as a model drug at a fixed compression force. Based on the tablet hardness observed in this study, MK-MCC effectively accommodated 50% paracetamol. Both MK-MCC and Avicel PH 101 exhibit similar dilution capacities for the model drug used.

4.3.3.6. Calibration Curve of directly compressed Paracetamol Tablet

A stock solution of paracetamol at 200 µg/ml in phosphate buffer (pH 5.8) was prepared. A standard calibration curve was generated using nine different concentrations (in µg/ml) of paracetamol. The absorbance values at 243 nm were plotted against the concentrations of the solutions (Figure 20). A linear regression analysis produced a calibration curve with the equation Y = 0.0562857X - 0.0120 (where Y represents absorbance and X represents concentration in µg/ml), and a correlation coefficient of 0.999.

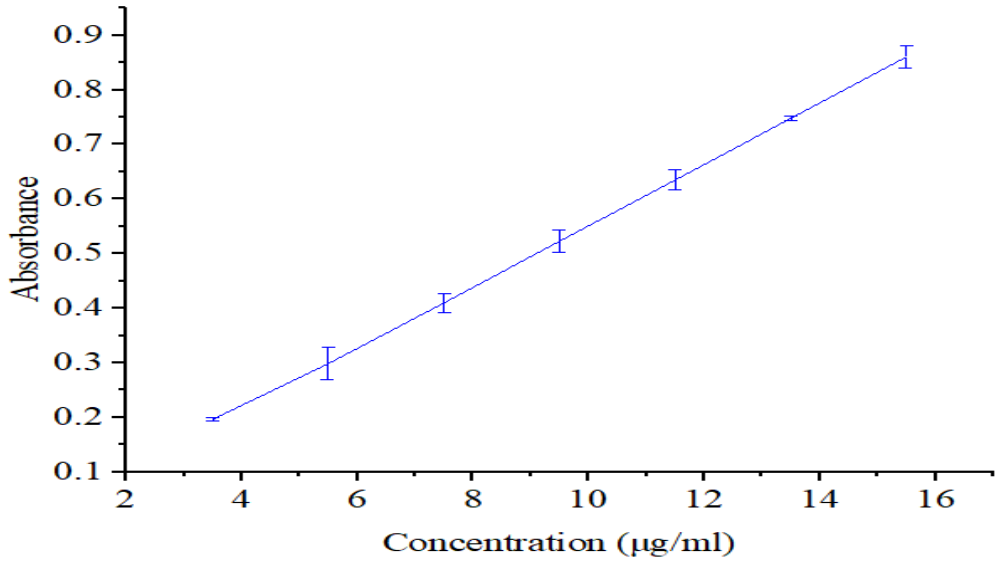

Figure 22: Absorbance of paracetamol in phosphate buffer (pH 5.8) at 243 nm

4.3.3.7. *Invitro* Drug Dissolution Study

The dissolution rate of the paracetamol tablets at concentration of 35%, and 50% w/w prepared from MK-MCC and Avicel PH10 are given in figure 21. After 30 minutes of dissolution, MK-MCC tablets with 35% paracetamol released 92.5% ± 1.1 of the drug, whereas tablets made with Avicel PH101 released 90.2% ± 0.8 of the drug at the same paracetamol concentration. This could be due to difference of tablet hardness. MK-MCC and Avicel PH 101 tablet at 35% paracetamol concentration also released 96.9% ±1.0 and 95.4% ± 0.79 of drug after 45 minute dissolution process respectively (Figure 21). The MK-MCC tablets had significantly rapid disintegration rate than that of Avicel PH 101 at all level of paracetamol concentration ($p < 0.05$). As the paracetamol concentration increased, the amount of paracetamol released from

the tablets during the 45 minute dissolution period also increased. This increased rate of dissolution could be attributed to a reduction in the tablet's hardness (Ghayas et al., 2013). According to USP 30/NF 25, 2007 standards, tablets should release over 80% of their content within 30 minutes and more than 90% within 45 minutes. Both MK-MCC and Avicel PH 101 tablets met these requirements. A significant difference was observed in the dissolution profiles of paracetamol tablets formulated with MK-MCC compared to those made with Avicel PH 101 powders ($p<0.05$). This discrepancy could also be due to differences in tablet hardness (Long and Chen, 2009).

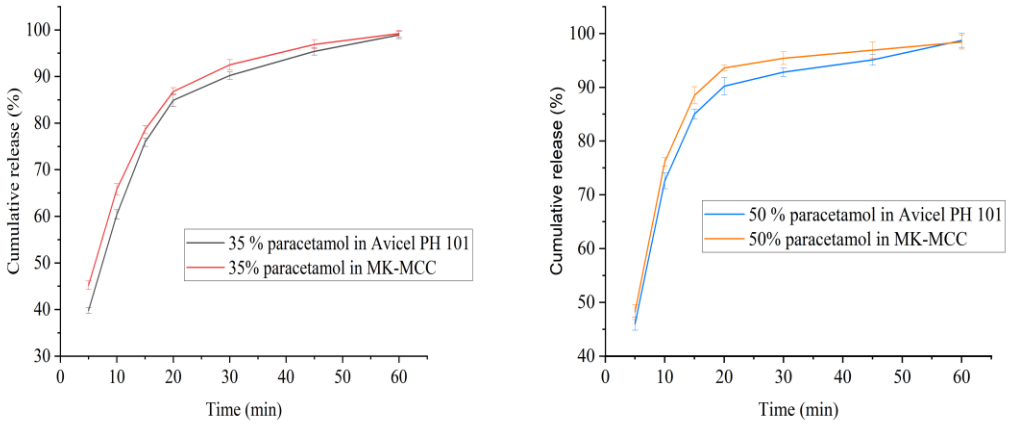

Figure 23: Dissolution profiles of MK-MCC tablets containing 35% and 50% paracetamol

CONCLUSIONS

Cellulose and microcrystalline cellulose were effectively isolated from mango kernel fiber using an alkaline treatment method with comparable yield to commonly reported values in the literature. The isolated MK-MCC was characterized with SEM, FTIR, XRD, TGA & DTA. MK-MCC exhibited comparable FTIR spectra with Avicel PH 101. The SEM analysis of MK-MCC was almost identical to that of Avicel PH-101. Moisture content, ash value, pH, water soluble substances, ether soluble substances, DP, density, mean particle size and particle size distribution of MK-MCC agreed with the values set for Avicel PH-101. MK-MCC was able to accommodate 50% of paracetamol with acceptable crushing strength, tensile strength, friability, disintegration, and in-vitro drug release properties at fixed compression force. The MK-MCC met almost all required characteristics of pharmaceutical excipients and that mango kernel waste is abundantly available as a byproduct. Therefore, it is possible to conclude that MCC from mango kernel can be promising alternative sources of MCC for pharmaceutical applications.

SUGGESTIONS FOR FUTURE WORK

Further work should be undertaken on the following:

- Optimization of cellulose and MCC preparation processes (like hydrolysis conditions, post hydrolysis milling condition)
- Evaluate MCC as a diluent in tablets made by wet granulation method as well as a filler for capsules
- Studies on the stability of tablets prepared from MCC powder over both short and long terms.

REFFERENCE

ADELEYE, O. A., BAMIRO, O. A., ALBALAWI, D. A., ALOTAIBI, A. S., IQBAL, H., SANYAOLU, S., FEMI-OYEWO, M. N., SODEINDE, K. O., YAHAYA, Z. S. & THIRIPURANATHAR, G. 2022. Characterizations of alpha-cellulose and microcrystalline cellulose isolated from cocoa pod husk as a potential pharmaceutical excipient. *Materials,15(17),*1-17

ALFA, J. 2008. Effect of lubricants on flow properties and tablet strength of silicified microcrystalline cellulose, *Pharm. Sci.,* 33, 71–75

ARNATA, I. W., FAHMA, F., RICHANA, N. & SUNARTI, T. C. 2019. Cellulose Production from Sago Frond with Alkaline Delignification and Bleaching on Various Types of Bleach Agents. *Oriental Journal of Chemistry*, 35 (1), 8-19.

ASIF, M., AHMED, D., AHMAD, N., QAMAR, M. T., ALRUWAILI, N. K. & BUKHARI, S. N. A. 2022. Extraction and characterization of microcrystalline cellulose from Lagenaria siceraria fruit pedicles. *Polymers,* 14(9)**.**

AZIZ, T., FARID, A., HAQ, F., KIRAN, M., ULLAH, A., ZHANG, K., LI, C., GHAZANFAR, S., SUN, H. & ULLAH, R. 2022. A review on the modification of cellulose and its applications. *Polymers,* 14(15).

BEGAT, P., PRICE, R., HARRIS, H., MORTON, D. A. & STANIFORTH, J. N. 2005. The influence of force control agents on the cohesive-adhesive balance in dry powder inhaler formulations. *KONA Powder and Particle Journal*, 23**,** 109-121.

BHATIA, S. K., JAGTAP, S. S., BEDEKAR, A. A., BHATIA, R. K., PATEL, A. K., PANT, D., BANU, J. R., RAO, C. V., KIM, Y.-G. & YANG, Y.-H. 2020. Recent developments in pretreatment technologies on lignocellulosic biomass: effect of key parameters, technological improvements, and challenges. *Bioresource technology,* 300.

CHAERUNISAA, A. Y., SRIWIDODO, S. & ABDASSAH, M. 2019. Microcrystalline cellulose as pharmaceutical excipient. *Pharmaceutical formulation design-recent practices.* Usama Ahmad, Juber Akhtar, IntechOpen. 41-54,

CHOUDHARY, P., DEVI, T. B., TUSHIR, S., KASANA, R. C., POPATRAO, D. S. & K, N. 2023. Mango seed kernel: A bountiful source of nutritional and bioactive compounds. *Food and Bioprocess Technology,* 16**,** 289-312.

CIOLACU, D., CIOLACU, F. & POPA, V. I. 2011. Amorphous cellulose—structure and characterization. *Cellulose chemistry and technology,* 45(1)**,** 13-21.

COLLARD, F.-X. & BLIN, J. 2014. A review on pyrolysis of biomass constituents: Mechanisms and composition of the products obtained from the conversion of cellulose, hemicelluloses and lignin. *Renewable and sustainable energy reviews,* 38**,** 594-608.

COLLAZO-BIGLIARDI, S., ORTEGA-TORO, R. & BOIX, A. C. 2018. Isolation and characterisation of microcrystalline cellulose and cellulose nanocrystals from coffee husk and comparative study with rice husk. *Carbohydrate polymers,* 191**,** 205-215.

DAS, K., RAY, D., BANDYOPADHYAY, N. & SENGUPTA, S. 2010. Study of the properties of microcrystalline cellulose particles from different renewable resources by XRD, FTIR, nanoindentation, TGA and SEM. *Journal of Polymers and the Environment,* 18**,** 355-363.

DONNER, M., GOHIER, R. & DE VRIES, H. 2020. A new circular business model typology for creating value from agro-waste. *Science of the Total Environment,* 716**,** 1-13.

EJIKEME, P. M. 2008. Investigation of the physicochemical properties of microcrystalline cellulose from agricultural wastes I: Orange mesocarp. *Cellulose,* 15**,** 141-147.

GABRIEL, T., BELETE, A., SYROWATKA, F., NEUBERT, R. H. & GEBRE-MARIAM, T. 2020. Extraction and characterization of celluloses from various plant byproducts. *International journal of biological macromolecules,* 158**,** 1248-1258.

GAMBLE, J. F., CHIU, W.-S. & TOBYN, M. 2011. Investigation into the impact of sub-populations of agglomerates on the particle size distribution and flow properties of conventional microcrystalline cellulose grades. *Pharmaceutical development and technology,* 16**,** 542-548.

GANESHAN, G., SHADANGI, K. P. & MOHANTY, K. 2016. Thermo-chemical conversion of mango seed kernel and shell to value added products. *Journal of Analytical and Applied Pyrolysis,* 121**,** 403-408.

GBENGA, B. L. & FATIMAH, O. F. 2014. Investigation of [alpha]-Cellulose Content of Sugarcane Scrappings and Bagasse as Tablet Disintegrant. *Journal of Basic & Applied Sciences,* 10**,** 142-148.

GETACHEW, M., GABRIEL, T., BELETE, A. & GEBRE-MARIAM, T. 2023. Extraction and characterization of cellulose and microcrystalline cellulose from Teff straw and evaluation of the microcrystalline cellulose as tablet excipient. *Journal of Natural Fibers,* 20(2).

GHAYAS, S., SHERAZ, M., ANJUM, F. & BAIG, M. T. 2013. Factors influencing the dissolution testing of drugs. *Pakistan Journal of Medical Research,* 1(1)**,** 1-11.

GUPTA, P. K., RAGHUNATH, S. S., PRASANNA, D. V., VENKAT, P., SHREE, V., CHITHANANTHAN, C., CHOUDHARY, S., SURENDER, K. & GEETHA, K. 2019. An update on overview of cellulose, its structure and applications. *Cellulose*, 201**,** 59-81.

HAAFIZ, M. M., HASSAN, A., ZAKARIA, Z. & INUWA, I. 2014. Isolation and characterization of cellulose nanowhiskers from oil palm biomass microcrystalline cellulose. *Carbohydrate polymers,* 103**,** 119-125.

HALDAR, D. & PURKAIT, M. K. 2021. A review on the environment-friendly emerging techniques for pretreatment of lignocellulosic biomass: Mechanistic insight and advancements. *Chemosphere*, 264(2)**,** 1-16.

HARINI, K. & MOHAN, C. C. 2020. Isolation and characterization of micro and nanocrystalline cellulose fibers from the walnut shell, corncob and sugarcane bagasse. *International Journal of Biological Macromolecules,* 163**,** 1375-1383.

HEINZE, T. 2016. Cellulose: structure and properties. *Cellulose chemistry and properties: fibers, nanocelluloses and advanced materials***,** Springer, Cham, **271,** 1-52.

HEISE, K., DELEPIERRE, G., KING, A. W., KOSTIAINEN, M. A., ZOPPE, J., WEDER, C. & KONTTURI, E. 2021. Chemical modification of reducing end-groups in cellulose nanocrystals. *Angewandte Chemie International Edition,* 60(1)**,** 66-87.

HENG, P. W. S., LIEW, C. V. & SOH, J. L. P. 2004. Pre-formulation studies on moisture absorption in microcrystalline cellulose using differential thermo-gravimetric analysis. *Chemical and pharmaceutical bulletin,* 52(4)**,** 384-390.

HON, D. N.-S. 2017. Chemical modification of cellulose. *Chemical modification of lignocellulosic materials.* Routledge. 31-60

HONJA, T. 2014. Review of mango value chain in Ethiopia. *Journal of Biology, Agriculture and Healthcare,* 4(25)**,** 230-239.

HUBBELL, C. A. & RAGAUSKAS, A. J. 2010. Effect of acid-chlorite delignification on cellulose degree of polymerization. *Bioresource technology,* 101(19)**,** 7410-7415.

JAHURUL, M., ZAIDUL, I., GHAFOOR, K., AL-JUHAIMI, F. Y., NYAM, K.-L., NORULAINI, N., SAHENA, F. & OMAR, A. M. 2015. Mango (Mangifera indica L.) by-products and their valuable components: A review. *Food chemistry,* 183**,** 173-180.

KALIA, S., THAKUR, K., KUMAR, A. & CELLI, A. 2014. Laccase-assisted surface functionalization of lignocellulosics. *Journal of Molecular Catalysis B: Enzymatic,* 102**,** 48-58.

KAMBLI, N. D., MAGESHWARAN, V., PATIL, P. G., SAXENA, S. & DESHMUKH, R. R. 2017. Synthesis and characterization of microcrystalline cellulose powder from corn husk fibres using bio-chemical route. *Cellulose,* 24**,** 5355-5369.

KARIMI, K., SHAFIEI, M. & KUMAR, R. 2013. Progress in physical and chemical pretreatment of lignocellulosic biomass. *Biofuel technologies: recent developments.* Springer, Berlin, Heidelberg, 53-96

KATAKOJWALA, R. & MOHAN, S. V. 2020. Microcrystalline cellulose production from sugarcane bagasse: Sustainable process development and life cycle assessment. *Journal of Cleaner Production,* 249**,** 1-50.

KIM, U.-J., EOM, S. H. & WADA, M. 2010. Thermal decomposition of native cellulose: influence on crystallite size. *Polymer Degradation and Stability,* 95**,** 778-781.

KONDO, T. 2005. Hydrogen bonds in cellulose and cellulose derivatives. *Polysaccharides: Structural diversity and functional versatility***,** CRC PRESS, 69-98.

KOTHARI, S. H., KUMAR, V. & BANKER, G. S. 2002. Comparative evaluations of powder and mechanical properties of low crystallinity celluloses, microcrystalline celluloses, and powdered celluloses. *International Journal of Pharmaceutics,* 232(1-2)**,** 69-80.

KUMAR, V., KOTHARI, S. H. & BANKER, G. S. 2001. Compression, compaction, and disintegration properties of low crystallinity celluloses produced using different agitation rates during their regeneration from phosphoric acid solutions. *AAPS PharmSciTech,* 2**,** 22-28.

KUNUSA, W. R., ISA, I., LALIYO, L. A. & IYABU, H. 2018. FTIR, XRD and SEM analysis of microcrystalline cellulose (MCC) fibers from corncorbs in alkaline treatment. *Journal of Physics: Conference Series,*. IOP Publishing, 1028.

LAVANYA, D., KULKARNI, P., DIXIT, M., RAAVI, P. K. & KRISHNA, L. N. V. 2011. Sources of cellulose and their applications—A review. *International Journal of Drug Formulation and Research,* 2**,** 19-38.

LEE, W. B., WIDJAJA, E., HENG, P. W. S. & CHAN, L. W. 2019. Near infrared spectroscopy for rapid and in-line detection of particle size distribution variability in lactose during mixing. *International Journal of Pharmaceutics,* 566**,** 454-462.

LI, J., WANG, Z., XIU, H., ZHAO, X., MA, F., LIU, L., YI, C., ZHANG, M., KOZLIAK, E. & JI, Y. 2022. Correlation between the powder characteristics and particle morphology of microcrystalline cellulose (MCC) and its tablet application performance. *Powder Technology,* 399.

LIEBERT, T. & KLEMM, D. 1998. A new soluble and hydrolytically cleavable intermediate in cellulose functionalization: cellulose dichloroacetate (CDCA). *Acta polymerica,* 49**,** 124-128.

LONG, M. & CHEN, Y. 2009. Dissolution testing of solid products. *Developing solid oral dosage forms.* Editor(s): Yihong Qiu, Yisheng Chen, Geoff G.Z. Zhang, Lirong Liu, William R. Porter, Academic Press, 319-340.

MALLAH, M. A., SHERAZI, S. T. H., BHANGER, M. I., MAHESAR, S. A. & BAJEER, M. A. 2015. A rapid Fourier-transform infrared (FTIR) spectroscopic method for direct

quantification of paracetamol content in solid pharmaceutical formulations. *Spectrochimica Acta Part A: Molecular and Biomolecular Spectroscopy,* 141**,** 64-70.

MARTINELLI, A., GIANNINI, L. & BRANDUARDI, P. 2021. Enzymatic modification of cellulose to unlock its exploitation in advanced materials. *ChemBioChem,* 22**,** 974-981.

MIHRANYAN, A., LLAGOSTERA, A. P., KARMHAG, R., STRØMME, M. & EK, R. 2004. Moisture sorption by cellulose powders of varying crystallinity. *International journal of pharmaceutics,* 269**,** 433-442.

NASATTO, P. L., PIGNON, F., SILVEIRA, J. L., DUARTE, M. E. R., NOSEDA, M. D. & RINAUDO, M. 2015. Methylcellulose, a cellulose derivative with original physical properties and extended applications. *Polymers,* 7**,** 777-803.

NG, C. H. 2019. Extraction, isolation, characterization and applications of cellulose derived from orange peel, Doctoral dissertation, UTAR, 106-126

NORRRAHIM, M. N. F., ILYAS, R. A., NURAZZI, N. M., RANI, M. S. A., ATIKAH, M. S. N. & SHAZLEEN, S. S. 2021. Chemical pretreatment of lignocellulosic biomass for the production of bioproducts: an overview. *Applied Science and Engineering Progress,* 14**,** 588-605.

NWACHUKWU, N. & OFOEFULE, S. I. EFFECT OF DRYING METHODS ON THE POWDER AND COMPACTION PROPERTIES OF MICROCRYSTALLINE CELLULOSE DERIVED FROM BAMBUSA VULGARIS, *European Journal of Pharmaceutical and Medical Research,* 6(9), 178-193.

NWADIOGB, J., IGWE, A., OKOYE, N. & CHIME, C. 2015. Extraction and characterization of microcrystalline cellulose from mango kernel: A waste management approach. *Scholars Research Library Der Pharma Chemica,* 7(11), 1-7

OBERLERCHNER, J. T., ROSENAU, T. & POTTHAST, A. 2015. Overview of methods for the direct molar mass determination of cellulose. *Molecules,* 20**,** 10313-10341.

OHWOAVWORHUA, F. & ADELAKUN, T. 2005. Some physical characteristics of microcrystalline cellulose obtained from raw cotton of Cochlospermum planchonii. *Tropical Journal of Pharmaceutical Research,* 4**,** 501-507.

OSEI-YEBOAH, F. & SUN, C. C. 2015. Validation and applications of an expedited tablet friability method. *International journal of pharmaceutics,* 484**,** 146-155.

PACHUAU, L., MALSAWMTLUANGI, C., NATH, N. K., RAMDINSANGI, H., VANLALFAKAWMA, D. C. & TRIPATHI, S. K. 2013. Physicochemical and functional characterization of microcrystalline cellulose from bamboo (Dendrocalamus longispathus). *International Journal of PharmTech Research,* 5**,** 1561-1571.

PACHUAU, L., VANLALFAKAWMA, D. C., TRIPATHI, S. K. & LALHLENMAWIA, H. 2014. Muli bamboo (Melocanna baccifera) as a new source of microcrystalline cellulose. *Journal of applied Pharmaceutical science,* 4(11)**,** 087-094.

PAUL, S. & SUN, C. C. 2017. Dependence of friability on tablet mechanical properties and a predictive approach for binary mixtures. *Pharmaceutical research,* 34**,** 2901-2909.

RAJANI, C., KUMAR, D. D., JAYA, D. & KUMAR, J. A. 2018. Effects of granule particle size and lubricant concentration on tablet hardness containing large concentration of polymers. *Brazilian Journal of Pharmaceutical Sciences,* 53(3).

ROWELL, R. M., PETTERSEN, R., HAN, J. S., ROWELL, J. S. & TSHABALALA, M. A. 2005. Cell wall chemistry. *Handbook of wood chemistry and wood composites,* 2**,** 33-72.

SAIGAL, N., BABOOTA, S., AHUJA, A. & ALI, J. 2009. Microcrystalline cellulose as a versatile excipient in drug research. *Journal of Young Pharmacists,* 1(1)**,** 1-7.

SAINORUDIN, M. H., MOHAMMAD, M., KADIR, N. H. A., ABDULLAH, N. A. & YAAKOB, Z. 2018. Characterization of several microcrystalline cellulose (Mcc)-based agricultural wastes via x-ray diffraction method. *Solid state phenomena,* 280**,** 340-345.

SALEM, K. S., KASERA, N. K., RAHMAN, M. A., JAMEEL, H., HABIBI, Y., EICHHORN, S. J., FRENCH, A. D., PAL, L. & LUCIA, L. A. 2023. Comparison and assessment of methods for cellulose crystallinity determination. *Chemical Society Reviews*.**52**, 6417-6446

SARKIS, J., GONZALEZ-TORRE, P. & ADENSO-DIAZ, B. 2010. Stakeholder pressure and the adoption of environmental practices: The mediating effect of training. *Journal of operations Management,* 28**,** 163-176.

SENUSI, N. A., SHOHAIMI, N. A. M., AB HALIM, A. Z., SHUKR, N. M., RAZAB, M. K. A. A., MOHAMED, M., AMIN, M. A. M., MOKHTAR, W. N. A. W., ISMARDI, A. & ABDULLAH, N. H, 2020. Preparation & Characterization of Microcrystalline Cellulose from Agriculture Waste. *Earth and Environmental Science,*. IOP Publishing, 596(1).

SHAH, R. B., TAWAKKUL, M. A. & KHAN, M. A. 2008. Comparative evaluation of flow for pharmaceutical powders and granules. *Aaps Pharmscitech*, 9**,** 250-258.

SHLIEOUT, G., ARNOLD, K. & MÜLLER, G. 2002. Powder and mechanical properties of microcrystalline cellulose with different degrees of polymerization. *Aaps Pharmscitech,* 3**,** 45-54.

SHOKRI, J. & ADIBKIA, K. 2013. Application of cellulose and cellulose derivatives in pharmaceutical industries. *Cellulose-medical, pharmaceutical and electronic applications.* IntechOpen.

SINDHU, R., BINOD, P. & PANDEY, A. 2016. Biological pretreatment of lignocellulosic biomass–An overview. *Bioresource technology,* 199**,** 76-82.

SINDHU, R., PANDEY, A. & BINOD, P. 2015. Alkaline treatment. *Pretreatment of biomass.* 51-60.

SOHNI, S., BEGUM, S., HASHIM, R., KHAN, S. B., MAZHAR, F., SYED, F. & KHAN, S. A. 2024. Physicochemical characterization of microcrystalline cellulose derived from underutilized orange peel waste as a sustainable resource under biorefinery concept. *Bioresource Technology Reports,* 25.

SPIRIDON, I. & POPA, V. I. 2008. Hemicelluloses: major sources, properties and applications. Editor(s): Mohamed Naceur Belgacem, Alessandro Gandini, *Monomers, polymers and composites from renewable resources.* Elsevier, 289-304.

SUNDARRAJ, A. A. & RANGANATHAN, T. V. 2018. A review on cellulose and its utilization from agro-industrial waste. *Drug Invent. Today,* 10**,** 89-94.

TAN, G., AV MORTON, D. & LARSON, I. 2015. On the methods to measure powder flow. *Current pharmaceutical design,* 21**,** 5751-5765.

TESSEMA, T. A., FEROCHE, A. T., WORKNEH, G. A. & GABRIEL, T. 2023. Physicochemical characterization of cellulose and microcrystalline cellulose from Cordia africana lam. seeds. *Journal of Natural Fibers,* 20(2)**,** 1-12.

THARANATHAN, R., YASHODA, H. & PRABHA, T. 2006. Mango (Mangifera indica L.),"The king of fruits"—An overview. *Food reviews international,* 22(2)**,** 95-123.

THIELEMANS, K., DE BONDT, Y., VAN DEN BOSCH, S., BAUTIL, A., ROYE, C., DENEYER, A., COURTIN, C. M. & SELS, B. F. 2022. Decreasing the degree of polymerization of microcrystalline cellulose by mechanical impact and acid hydrolysis. *Carbohydrate Polymers,* 294**,** 1-8.

TKACHEVA, N., MOROZOV, S., GRIGOR'EV, I., MOGNONOV, D. & KOLCHANOV, N. 2013. Modification of cellulose as a promising direction in the design of new materials. *Polymer Science Series B,* 55**,** 409-429.

TOMAR, M., KUMAR, S. A. & RAJ, S. A. 2017. Effect of moisture content of exicipient (microcrystalline cellulose) on direct compressible solid dosage forms. *International Journal of Pharmaceutical Sciences and Research,* 8(1)**,** 282-288.

TRACHE, D., DONNOT, A., KHIMECHE, K., BENELMIR, R. & BROSSE, N. 2014. Physico-chemical properties and thermal stability of microcrystalline cellulose isolated from Alfa fibres. *Carbohydrate polymers,* 104**,** 223-230.

TRACHE, D., HUSSIN, M. H., CHUIN, C. T. H., SABAR, S., FAZITA, M. N., TAIWO, O. F., HASSAN, T. & HAAFIZ, M. M. 2016. Microcrystalline cellulose: Isolation, characterization and bio-composites application—A review. *International Journal of Biological Macromolecules,* 93**,** 789-804.

TRACHE, D., KHIMECHE, K., DONNOT, A. & BENELMIR, R, 2013.. FTIR spectroscopy and X-ray powder diffraction characterization of microcrystalline cellulose obtained from alfa fibers. *MATEC Web of Conferences, EDP Sciences,* 3(1)

USP, U. 30, NF 25. The United States Pharmacopeia and The National Formulary, The United States Pharmacopoeial Convention, INC, 2007.

VASSILEV, S. V., BAXTER, D., ANDERSEN, L. K., VASSILEVA, C. G. & MORGAN, T. J. 2012. An overview of the organic and inorganic phase composition of biomass. *Fuel,* 94**,** 1-33.

VERONICA, N., HENG, P. W. S. & LIEW, C. V. 2022. Relative humidity cycling: implications on the stability of moisture-sensitive drugs in solid pharmaceutical products. *Molecular Pharmaceutics,* 20**,** 1072-1085.

WANG, J., WEN, H. & DESAI, D. 2010. Lubrication in tablet formulations. *European journal of pharmaceutics and biopharmaceutics,* 75**,** 1-15.

WERNER, K., POMMER, L. & BROSTRÖM, M. 2014. Thermal decomposition of hemicelluloses. *Journal of Analytical and Applied Pyrolysis,* 110**,** 130-137.

YASSIN, S., GOODWIN, D. J., ANDERSON, A., SIBIK, J., WILSON, D. I., GLADDEN, L. F. & ZEITLER, J. A. 2015. The disintegration process in microcrystalline cellulose based tablets, part 1: influence of temperature, porosity and superdisintegrants. *Journal of Pharmaceutical Sciences,* 104**,** 3440-3450.

ZHAO, H., ZHAO, L., LIN, X. & SHEN, L. 2022. An update on microcrystalline cellulose in direct compression: Functionality, critical material attributes, and co-processed excipients. *Carbohydrate Polymers,* 278**.**

ZHENG, Y., ZHAO, J., XU, F. & LI, Y. 2014. Pretreatment of lignocellulosic biomass for enhanced biogas production. *Progress in energy and combustion science,* 42**,** 35-53.

ZULIAHANI, A., NURUL NADHIRAH, R., ROZYANTY, A., NAWAWI, W. I. & NOR HANANI, A. 2016. Crystallinity, tapping and bulk density of microcrystalline cellulose (MCC) isolated from rice husk (RH). *Applied Mechanics and Materials,* 835**,** 272-276.